Studies on calcium signaling mechanisms at fertilization and activation of mouse eggs

マウス卵の受精および活性化における
カルシウムシグナリング機構
に関する研究

Kei Sugo

須郷　圭

Studies on calcium signaling mechanisms at fertilization and activation of mouse eggs

マウス卵の受精および活性化における
カルシウムシグナリング機構
に関する研究

Kei Suga

須賀　圭

Contents

Abbreviation

4-Br A23187	4-bromo A23187
AM	Acetoxymethyl ester
ATP	Adenosine 5'-triphosphate
BAPTA	1,2-bis-(*o*-Aminophenoxy)ethane-tetraacetic acid
BHQ	2,5-di-(*tert*-Butyl)-1,4-hydroquinone
BSA	Bovine serum albumin
Ca^{2+}	Calcium ion
$[Ca^{2+}]_i$	Intracellular Ca^{2+} concentration
CCE	Capacitative calcium entry
CG	Cortical granule
CICR	Calcium-induced calcium release
DIC	Differential interference contrast
DMSO	Dimethyl sulfoxide
DTT	Dithiothreitol
EGTA	[ethylenebis-(oxyethylenenitrilo)] tetraacetic acid
ER	Endoplasmic reticulum
FITC	Fluorescein isothiocyanate
GTP	Guanosine 5'-triphosphate
hCG	Human chorionic gonadotropin
HEPES	N-2-hydroxyethylpiperazine-N'-2-ethanesulfonic acid
HR	Hyperpolarizing response
IICR	Inositol 1,4,5-trisphosphate-induced calcium release
IP_3	Inositol 1,4,5-trisphosphate
IP_3R	Inositol 1,4,5-trisphosphate receptor
IP_3R-1	Inositol 1,4,5-trisphosphate receptor type 1
IP_3R-2	Inositol 1,4,5-trisphosphate receptor type 2
IP_3R-3	Inositol 1,4,5-trisphosphate receptor type 3

IVF	*In vitro* fertilization
LCA	*Lens culinaris agglutinin*
mAb	Monoclonal antibody
Mg^{2+}	Magnesium ion
mRNA	Messenger ribonucleic acid
NAADP	Nicotinic-acid adenine dinucleotide phosphate
Ni^{2+}	Nickel ion
PB	Polar body
PBS	Phosphate-buffered saline
PIP_2	Phosphatidylinositol 4,5-bisphosphate
PLC	Phospholipase C
PKC	Protein kinase C
PMCA	Plasma membrane Ca^{2+}-ATPase
PMSF	Phenylmethylsulfonyl fluoride
PMSG	Pregnant mare's serum gonadotropin
PN	Pro-nucleus
PVA	Polyvinylalcohol
PVDF	Polyvinylidene difluoride
PVP	Polyvinylpyrrolidone
R	Ratio (F340/F380)
R_{peak}	Maximal peak ratio
RyR	Ryanodine receptor
S.D.	Standard deviation
SDS	Sodium dodecylsulfate
SDS-PAGE	SDS polyacrylamide gel electrophoresis
SERCA	Sarcoplasmic reticulum calcium ATPase
SIT	Silicone-intensified target
SR	Sarcoplasmic reticulum
Sr^{2+}	Strontium ion

TG	Thapsigargin
TMS	Thimerosal (ethylmercurithiosalicylate)
Tris	Tris[hydroxyethyl]aminoethane
TRS	Tyrode ringer's saline
TYH	Toyoda, Yokoyama, Hoshi
ZP	*Zonae pellucidae*

Abstract

Precise function and consequences of Ca^{2+} oscillations and signaling of Ca^{2+} that leads to the cellular functions after fertilization of mouse egg are remaining problems to be solved.

In this study, in order to investigate the underlying mechanisms of Ca^{2+} signaling in mature mouse egg, I focused on the two phenomena: Ca^{2+} oscillation and cortical granule exocytosis that occur after fertilization by sperm. To define the role of Ca^{2+}-ATPase and Ca^{2+} influx pathway at Ca^{2+} oscillations in mouse eggs, I applied Ca^{2+}-ATPase inhibitors and an antagonist for capacitative calcium entry in conjunction with other reagents inducing Ca^{2+} oscillations such as thimerosal and with fertilizing sperm. I used two chemically unrelated Ca^{2+}-ATPase inhibitors thapsigargin and 2,5-di-(*tert*-butyl)-1,4-hydroquinone (BHQ) and an antagonist for capacitative calcium entry SK&F 96365 as tools to study the mechanism pharmacologically. Moreover, using Ca^{2+}-ATPase inhibitors, dependence of cortical granule exocytosis on Ca^{2+} change in the egg cytoplasm was examined.

In chapter I, results from immunoblotting and immunohistochemical experiments using subtype specific monoclonal antibodies to the IP_3 receptors (IP_3Rs) indicated that the type 1 IP_3 receptor (IP_3R-1) was predominantly expressed and localized in the cortex as clusters in mature mouse eggs. These results suggest that among the intracellular Ca^{2+} release channels, type 1 IP_3R may solely functions as a molecular base in the Ca^{2+} release mechanism at fertilization of mouse egg.

In chapter II, functional analysis of Ca^{2+} signaling in mouse egg was performed by loading fluorescent calcium indicator fura-2 into the eggs and measurment of intracellular Ca^{2+} concentration was done by Ca^{2+} imaging technique. I showed that two potent Ca^{2+}-ATPase inhibitors; thapsigargin and BHQ both showed a transient rise in $[Ca^{2+}]_i$ due to increase in leakage of Ca^{2+}

from the same Ca^{2+} store. At the concentration that cause maximal Ca^{2+} release, two inhibitors appeared to be possessing different activity upon divalent cation entry across the membrane. Depletion of the Ca^{2+} stores by thapsigargin induced divalent cation entry across the membrane. In contrast to thapsigargin, eggs treated with BHQ did not show such Ca^{2+} influx. The Ca^{2+} influx pathway activated by thapsigargin was sensitive to SK&F 96365 (an antagonist for capacitative calcium entry), since Ca^{2+} influx induced by thapsigargin was inhibited by the antagonist. These phenomena, shown above, are generally accepted as evidence of capacitative calcium entry. These results suggest that intrinsic mechanism that coupled with the depletion of the thapsigargin (and BHQ)-sensitive Ca^{2+} store and activation of Ca^{2+} influx is present in the mature mouse eggs and may work during Ca^{2+} oscillations at fertilization. When eggs showing repetitive Ca^{2+} transient were treated with the antagonist SK&F 96365, frequency of the Ca^{2+} oscillation decreased dose-dependently. These results suggest that Ca^{2+} influx activated by the depletion of the Ca^{2+} store operates at Ca^{2+} oscillation and that this influx is due to Ca^{2+} channel sensitive to SK&F 96365. Moreover, these results indicate that the frequency of oscillation is regulated, at least in part, by the Ca^{2+} influx from extracellular fluid. The effect of Ca^{2+}-ATPase inhibitors on Ca^{2+} oscillations was examined. Thapsigargin and BHQ both showed inhibitory effect on the Ca^{2+} oscillation induced by thimerosal in the presence and absence of extracellular Ca^{2+}. Moreover, Ca^{2+} oscillation induced by sperm was suppressed by the inhibitors. These results indicate that in mature mouse egg, Ca^{2+} pump sensitive to thapsigargin and BHQ exists and functions during Ca^{2+} oscillation induced by thimerosal and sperm. Above results suggest that Ca^{2+} oscillation in mouse egg is a modulated release of Ca^{2+} from the type 1 IP_3R localized in the cortex and the refilling of Ca^{2+} stores via thapsigargin- (and BHQ-) sensitive Ca^{2+}-ATPase and the Ca^{2+} influx via undefined Ca^{2+} channel but sensitive to SK&F 96365.

In chapter III, I found that the treatment of mature mouse eggs with Ca^{2+}-ATPase inhibitors triggered cortical granule (CG) exocytosis. This result provides the supportive evidence that CG exocytosis can be triggered by the transient increase in Ca^{2+} concentration in the cytosol. The Ca^{2+}-ATPase inhibitors will be very useful to control the Ca^{2+} concentration in the cyotsol and examine the threshold of Ca^{2+} concentration that triggers the CG exocytosis.

Introduction

Fertilization of mammalian eggs initiates a series of responses in the eggs that are temporally classified as "early" and "late" events of egg activation (Schultz and Kopf, 1995). Early events include a transient increase in intracellular Ca^{2+} concentration that leads to cortical granule (CG) exocytosis. The contents released from the CGs modify the *zonae pellucidae* (ZP) and result in a block to polyspermy. Late events of egg activation include the emmision of the second polar body (PB), recruitment of maternal mRNAs (Cascio and Wassarman, 1982) and posttranslational modifications of proteins (Van Blerkom, 1981; Endo *et al.*, 1986; Howlett, 1986), pronucleus (PN) formation and initiation of DNA synthesis, and cleavage. It is quite clear that Ca^{2+} is the second messenger that plays a key role in signal transduction and cellular function at fertilization in various species because intracellular calcium concentration changes are induced by the sperm, are essential, and are sufficient for activating the egg (Jaffe *et al.*, 1983; Whitaker and Steinhardt, 1982; Bement, 1992).

Mammalian eggs exhibit repetitive rises in the cytoplasmic Ca^{2+} concentrations (Ca^{2+} oscillations), associated with propagating Ca^{2+} waves in the initial responses at fertilization. How the sperm generates the Ca^{2+} changes in the egg cytoplasm at fertilization is a remaining problem to be solved. At least two main ideas have been put forward for the signaling systems used by a sperm to trigger Ca^{2+} release in eggs at fertilization. One is a sperm receptor coupled to GTP-binding protein (G-protein)/phospholipase C (PLC) pathway (Turner *et al.*, 1986; Miyazaki, 1988) or a protein tyrosine kinase/PLC pathway (Ciapa and Epel, 1991) leading to production of inositol 1,4,5-trisphosphate (IP_3) and then to IP_3-induced Ca^{2+} release (IICR). The other is a pathway involving a cytosolic

factor derived from the sperm (recently named "Oscillin") through cytoplasmic continuity of the sperm and egg (Swann, 1990; Whitaker and Swann, 1993; Parrington *et al.*, 1996).

The precise function and consequences of these Ca^{2+} oscillations remain as unknown in mammalian eggs as they do in many somatic cell types that undergo prolonged Ca^{2+} oscillations (Berridge and Galione, 1988; Miyazaki, 1991; Sun *et al.*, 1992; Kline and Kline, 1992a). The Ca^{2+} oscillations now receive much attention and is thought to be of general importance in cell biology. In mammalian eggs, as in the most other animals, it appears that the temporal oscillations of $[Ca^{2+}]_i$ is based primary on the modulated release and re-uptake of Ca^{2+} from intracellular stores (Igusa and Miyazaki, 1983; Kline and Kline, 1992a). Recent studies using a functional blocking monoclonal antibody to the inositol 1,4,5-trisphosphate (IP_3) receptor (IP_3R)/Ca^{2+} release channel demonstrated direct evidence that IICR from intracellular stores operates at fertilization of the hamster egg and that IICR is essential in the initiation, propagation, and oscillation of the sperm-induced Ca^{2+} transients (Miyazaki *et al.*, 1992b). Sensitization of Ca^{2+}-induced Ca^{2+} release (CICR), on the other hand, is suggested to be both necessary and sufficient to explain oscillations (Igusa and Miyazaki, 1983; Swann, 1991).

Thimerosal, a sulfhydryl-reagent, mimics the large and persistent Ca^{2+} oscillations seen at fertilization most successfully, in both hamster and mouse eggs (Miyazaki *et al.*, 1992a; Swann, 1991; Swann, 1992). The effects of thimerosal suggested that altering the sensitivity of Ca^{2+} channels may of itself be sufficient to cause Ca^{2+} oscillations. It is also suggested that a sensitizing action of Ca^{2+} on the IP_3R, i.e., Ca^{2+}-sensitized IICR, can serve as a regenerative process of Ca^{2+} release and could be the basis for Ca^{2+} oscillations (Miyazaki *et al.*, 1992b). On the

other hand, undergoing of the repetitive Ca^{2+} oscillations must have a feature in the necessity to move Ca^{2+} between the cytosol and storage sites by sequestration, a process that is principally, perhaps exclusively, attributable to the action of Ca^{2+}-ATPase (SERCA pumps) (Missiaen *et al.*, 1991). Moreover, refilling of the Ca^{2+} store is also mediated by Ca^{2+} influx, since fertilized eggs devoid of extracellular Ca^{2+}, greatly reduced the frequency of Ca^{2+} transients (Kline and Kline, 1992b). Accordingly, inhibition of Ca^{2+}-ATPase and Ca^{2+} influx pathway should be disruptive to induced oscillations. However, the nature and regulation of Ca^{2+} re-uptake and Ca^{2+} entry pathways and signaling of Ca^{2+} that leads to the development of mouse eggs are still uncertain.

I focused on the two phenomena of the early events of mouse egg activation; Ca^{2+} oscillations and cortical granule (CG) exocytosis. The aim of this study was to investigate the role of Ca^{2+}-ATPase and Ca^{2+} entry pathway operating during Ca^{2+} oscillations and the relationship between the Ca^{2+} signal and triggering of cortical granule (CG) exocytosis and discuss the possible Ca^{2+} signaling mechanisms that might be involved in early events at fertilization and activation of mouse eggs.

Materials and methods

Media and reagents

The media used in these experiments are TYH medium and Ca^{2+}, Mg^{2+}-free TRS medium with minor modifications. The composition of TYH was 119.37 mM NaCl, 4.78 mM KCl, 1.71 mM $CaCl_2$, 1.19 mM KH_2PO_4, 1.19 mM $MgSO_4$, 25.07 mM $NaHCO_3$, 1 mM sodium pyruvate (Katayama kagaku, Osaka, Japan), 5.56 mM glucose (Sigma, MO, U.S.A.), 100 units/ml pennicilin G (Banyu, Tokyo, Japan), 50 μg/ml streptomycin sulphate (Meiji Seika Kaisha Ltd., Tokyo, Japan), 0.0002% phenol red (Life technologies, NY, U.S.A.) and 4 mg/ml bovine serum albumin (BSA, type V; Sigma). The composition of Ca^{2+}, Mg^{2+}-free TRS medium (pH 7.4) was 136.9 mM NaCl, 4.02 mM KCl, 0.44 mM NaH_2PO_4, 0.18 mM KH_2PO_4, 11.9 mM $NaHCO_3$, 11.1 mM glucose, 0.0002 % phenol red, 0.1 % polyvinylpyrolidone (Sigma).

Media were made with cell culture reagents and tissue culture grade water. All chemicals, except where noted, were obtained from Wako Pure Chemicals (Osaka, Japan). All media were filtered through 0.22 μm pore size filters (Type GV; Millipore, MA, U.S.A.) and equilibrated at 37 °C under mineral oil in an atmosphere of 5 % CO_2, 95 % air.

Materials

Fura-2 AM, calcium green-1 AM and 4-Br A23187 were purchased from Molecular Probes (OR, U.S.A.). U73122 were obtained from BIOMOL Research Laboratories (PA, U.S.A.). Thapsigargin and BHQ, (La Jolla, CA, U.S.A.). These drugs shown above were dissolved in DMSO (Sigma). SK&F 96365 were from Calbiochem. Thimerosal, DTT

and caffeine were all from Sigma. EGTA and HEPES were from Dojindo (Kumamoto, Japan).

Preparation of gametes

ICR female mice (8-12 weeks; SLC Japan, Hamamatsu, Japan) were superovulated by intraperitoneal injection of 7 i.u of pregnant mare's serum gonadotropin (PMSG; Sankyo, Tokyo, Japan) followed 48 hour later by 5 i.u of human chorionic gonadtropin (hCG; Sigma). Metaphase-II arrested eggs were released from the oviduct into warmed TYH medium containing 4 mg/ml BSA. Cumulus cells were removed by brief treatment with hyaluronidase (0.25 mg/ml; Type IV-S; Sigma) 15-16 hour post-hCG and washed four times with TYH medium. *Zonae pellucidae* (ZP) was removed by brief exposure (approximately 2 min) to α-chymotrypsin (2.5 μg/ml; Sigma) in TYH medium. After washing extensively with TYH medium, the eggs were drawn into and expelled from a small bore glass pipet, which aided in the removal of the ZP. Eggs were held in drops of TYH medium under mineral oil (Sigma) in tissue culture dishes. All manipulations were carried out at 37 °C on heated plates.

Sperm were expelled from the cauda epididymides of 12-15 weeks old male ICR (Clea Japan, Tokyo, and SLC Japan, Japan) mice into drops of TYH medium containing 4 mg/ml BSA. Sperm were diluted to 5 x 10^5 sperm/ml in TYH medium and incubated under mineral oil for at least 1.5 hour at 37 °C and 5% CO_2 to capacitate.

In vitro fertilization (IVF) and artificial activation

Eggs were inseminated in a 200 µl drop of TYH medium, under mineral oil. The final sperm concentration was 5-20 x 10^3 sperm/ml. Eggs were artificially activated by treatment with the Ca^{2+} ionophore 4-Br A23187 in Ca^{2+}, Mg^{2+}-free TRS medium. For ionophore activation, eggs were treated with 5 µM 4-Br A23187 for 2 min in Ca^{2+}, Mg^{2+}-free TRS medium, then washed and incubated in Ca^{2+}, Mg^{2+}-free TRS medium for 30 min.

Chapter I

IP_3 receptors in mouse egg

1. Introduction

Inositol 1,4,5-trisphosphate (IP_3) releases Ca^{2+} from intracellular stores by binding to an IP_3 receptor (IP_3R) (Supattapone *et al.*, 1988), which composes an IP_3-gated Ca^{2+} channel (Ferris *et al.*, 1989; Miyawaki *et al.*, 1990; Maeda *et al.*, 1991). Molecular cloning studies showed that there are at least three types of IP_3R subtypes derived from distinct genes, designated type 1 (IP_3R-1) (Furuichi *et al.*, 1989; Mignery *et al.*, 1990; Yamada *et al.*, 1994; Kume *et al.*, 1993), type 2 (IP_3R-2) (Sudhof *et al.*, 1991; Yoshikawa *et al.*, 1992; Yamamoto-Hino *et al.*, 1994), and type 3 (IP_3R-3) (Yamamoto-Hino *et al.*, 1994; Blondel *et al.*, 1993; Maranto, 1994). Recent studies using a functional blocking monoclonal antibody to the IP_3R demonstrated direct evidence that IP_3-induced Ca^{2+} release (IICR) from intracellular stores operates at fertilization of the hamster egg. IICR is essential in the initiation, propagation and oscillation of the sperm-induced Ca^{2+} increases. Ca^{2+}-induced Ca^{2+} release (CICR) has also been suggested, but a sensitizing action of Ca^{2+} on the IP_3R, i.e., Ca^{2+}-sensitized IICR, can serve as a regenerative process of Ca^{2+} release and could be the basis for Ca^{2+} waves and oscillations (Miyazaki *et al.*, 1992b; Miyazaki *et al.*, 1992a). These results indicate that the important role of IP_3R as molecular base in the Ca^{2+} signaling at fertilization and activation of mammalian eggs. It has been demonstrated that IP_3R-1 exists and functions in IP_3-induced Ca^{2+} release in mature mouse eggs (Mehlmann *et*

al., 1996). However, expression of other IP_3R subtypes have not been examined in mouse eggs.

In order to determine which subtypes of IP_3R are expressed in mature mouse eggs, I performed Western blot and immunohistochemical analysis using three different specific antibodies to each IP_3R subtypes.

2. Materials and methods

Antibodies

Rat monoclonal antibody 4C11 and 18A10 against mouse type 1 IP_3 receptor (IP_3R-1) were prepared as described previously (Maeda *et al.*, 1991). Mouse monoclonal antibodies KM1083 and KM1082 were raised against synthetic peptides corresponding to 15 C-terminal amino acids of IP_3R-2 (human IP_3R-2, 2687-2701) (Yamamoto-Hino *et al.*, 1994), and IP_3R-3 (human IP_3R-3, 2657-2771) (Yamamoto-Hino *et al.*, 1994), respectively. Detailed characterizations of these antibodies were described previously (Sugiyama *et al.*, 1994). Polyclonal antibody 908 was raised against synthetic peptide corresponding to 16 N-terminal amino acids of IP_3R-1 (mouse IP_3R-1, 40-55) (unpublished results).

Immunoblotting

Eggs were collected as described previously and the ZP was removed by a brief treatment in acidic Tyrode's solution (136.9 mM NaCl, 2.68 mM KCl, 1.63 mM $CaCl_2$, 0.73 mM $MgCl_2$, 5.55 mM glucose, 0.4 mg/ml polyvinylpyrrolidone, pH 2.5), followed by several washes through TYH medium. Cells were counted and washed in phosphate-buffered saline (PBS; pH 7.4), containing 0.1% polyvinylalcohol (PVA; Sigma) and transferred to a microcentrifuge tube. Most of the PBS was removed and lysing buffer (50 mM Tris-HCl, pH 6.8, 1 % sodium deoxycholate, 0.1% SDS, 0.8 mM phenylmethylsulfonyl fluoride, 10 μM leupeptin, 1 μM pepstatin A) were added and the cells were quickly frozen in liquid nitrogen and stored at -80 °C until use. Before loading the egg lysate into a polyacrylamide gel, one fifth volume of sample buffer (50 mM Tris-

HCl, pH 6.8, 50 % glycerol, 5 % SDS, 5 % 2-mercaptoethanol, 0.25 % pyronin Y) was added to each tube and the samples were incubated at 37 °C for 1 h. Membrane fraction of Raji cells, which all IP_3 receptor subtypes are expressed (Monkawa *et al.*, 1995), were used for comparison in immunoblotting experiments. Prior to loading in the gel, sample buffer was added to each aliquot and the mixture heated at about 65 °C for 20 min. Egg-lysate and membrane fraction of Raji cells were electrophoretically separated using a 4 % stacking, 5 % resolving polyacrylamide gel (Laemmli, 1970), followed by an overnight electrophoretic transfer to a PVDF membrane (Immobilon P; Millipore). Membranes were incubated in a blocking buffer (PBS, pH 7.4, 0.1 % Tween 20, 5 % nonfat milk) for 1 h and washed with PBS-T (PBS containing 0.1% Tween 20) followed by incubation with the primary antibodies for 90 min. Antibodies KM1083 and KM1082 were diluted in PBS-T to 4 μg/ml. For immunoblotting with 18A10 and 4C11, culture supernatant of hybridoma were used without dilution. Following primary antibody incubation, the membranes were washed four times for 5 min each with PBS-T and were incubated for 1 h with horseradish peroxidase-conjugated secondary antibody (anti-rat IgG from goat; Amersham, England) diluted 1:500 to PBS-T. After washing the membranes with PBS-T, labeled proteins were identified on X-ray film (Kodak, NY, U.S.A.) using an enhanced chemiluminescence method, according to the manufacture's protocol (ECL kit; Amersham).

Immunolocalization of the IP_3 receptors in eggs

Eggs were collected as described above and ZP was removed with a brief treatment (less than 3 min) with 2.5 μg/ml α-chymotrypsin. Following several washes through TYH medium, eggs were fixed for 30

min at 37 °C or over night at 4 °C in freshly prepared 3.7 % paraformaldehyde in PBS (pH 7.4) containing 0.1 % PVA. After fixation, eggs were washed three times (10 min) with PBS containing 0.1% PVA (PBS-PVA) and incubated with blocking buffer (PBS, pH 7.4, containing 3 % BSA and 0.25 % gelatin) for 15 min. Eggs were incubated in primary antibody for 90 min at 37 °C. Primary antibodies were 90 μg/ml of purified monoclonal antibody 4C11, KM1083 and KM1082 diluted in blocking buffer. Following primary antibody incubation, eggs were washed three times with blocking buffer and were incubated for 1 h with the secondary antibody (fluorescein-conjugated rabbit anti-rat IgG, Vector Laboratories, CA, U.S.A.) diluted in blocking buffer. Eggs were washed three times for 15 min in blocking buffer. Included in the first wash was 1 μg/ml Hoechst 33342 that allowed visualization of the position of the meiotic spindle in eggs. Eggs labeled by immunofluorescence were observed using standard epifluorescence microscopy or viewed with a laser-scanning confocal microscope (LSM410; Carl Zeiss). The eggs were washed into a drop of PBS before viewing. For examination with the confocal microscope, eggs were mounted on cover slides in PBS. Images of control eggs incubated with normal rat IgG (100 μg/ml) were made with the same excitation illumination intensity and viewed with the same confocal settings as eggs incubated with 4C11 antibody.

The method described above was established previously by Mehlmann (Mehlmann *et al.*, 1996). They showed that paraformaldehyde fixation alone, without permeabilization treatment, was sufficient to permit penetration of antibodies into the interior cytoplasm. Consistent with their result, I have also observed the penetration of the antibodies using antibody for ß-tublin as a control (data not shown).

3. Results

3.1 IP_3 receptors in mouse eggs

3.1.1 Western blotting of IP_3 receptors in eggs

Total lysate from 500 ZP-free eggs and membrane fraction of Raji cells for positive control were subjected to SDS-PAGE under reducing condition and transfered to PVDF membrane and probed with monoclonal antibodies (mAbs) 18A10 (for IP_3R-1), KM1083 (for IP_3R-2) and KM1082 (for IP_3R-3). As shown in Figure 1A (*lane* 2), IP_3R-1 immunoreactivity migrated as a band of approximately 240 kDa almost as same as positive control (*lane* 1). Although loaded egg lysate was overloaded and transferred membrane was over-exposed in order to detect the faint immunoreactive bands, immunoreactivity of IP_3R-2 (*lane* 4) and IP_3R-3 (*lane* 6) were not detected in this condition (Figure 1A). IP_3R-1 protein appeared on Western blots (Figure 1B) as a single band when each lane were loaded with 200 ZP-free eggs probed with another antibody for IP_3R-1; 4C11 (*lane* 1) and antibody 908 (*lane* 2) that may recognize all subtypes (unpublished results). Single band was also detected with mAb 18A10 in a lane loaded with approximately only 25 eggs (Figure 1C, *lane* 1). In contrast to IP_3R-2 and IP_3R-3, IP_3R-1 was predominantly expressed in mature mouse eggs.

3.1.2 Immunolocalization of the type 1 IP_3 receptors in eggs

To examine the spatial distribution of IP_3R-1 in mature mouse eggs, the localization of the IP_3R-1 was determined in four eggs using 4C11 antibody and laser-scanning confocal microscope as indicated under

Materials and Methods. As shown in Figure 2A, IP_3R-1 was organized in clusters and dispersed in the cortex and little staining was observed in the interior of the egg (Figure 2B). Similar staining pattern was observed in eggs from B6C3F1 mouse (n = 4; data not shown). Control eggs incubated with normal rat IgG (n = 2) for first antibody and the eggs without first antibody incubation (n = 2) did not show the same staining pattern observed in eggs stained with 4C11 (data not shown). Consisitent with the results from Western blot analysis, there was no specific immunoreactivity of IP_3R-2 and IP_3R-3 in the mature mouse egg, using KM1083 and KM1082 respectively (data not shown).

Above results, together with the results from Western blot analysis suggest that type 1 IP_3R may solely functions as a molecular base in the Ca^{2+} release mechanism at fertilization of mouse egg.

4. Discussion

4.1 IP_3 receptors in mouse eggs

Miyazaki et al. reported that monoclonal antibody to the IP_3R; 18A10 inhibited both IICR and CICR upon injection of IP_3 and Ca^{2+} into hamster eggs, respectively (Miyazaki *et al.*, 1992b). The 18A10 antibody completely blocked sperm-induced Ca^{2+} waves and oscillations. Moreover, this antibody blocked Ca^{2+} oscillations induced by thimerosal in the hamster egg (Miyazaki *et al.*, 1992a). In mouse eggs, it has been shown that heparin; known as antagonist to IP_3R blocked the Ca^{2+} oscillations (Kline and Kline, 1994), and 18A10 inhibited the IP_3-induced Ca^{2+} release (Mehlmann *et al.*, 1996). There is good evidence that Ca^{2+} release in the hamster and mouse egg is mediated solely by the IP_3R and that any apparent Ca^{2+}-induced Ca^{2+} release is mediated by sensitization of the IP_3-induced Ca^{2+} release by Ca^{2+}. Furthermore, functional analysis using caffeine (Figure 6) and the result from Kline et al. (Kline and Kline, 1994) revealed that no apparent property of caffeine-sensitive Ca^{2+} release exists in mature mouse eggs. Since functional blocking antibody; 18A10 is specific for type 1 IP_3R (IP_3R-1), complete inhibition of Ca^{2+} release with the antibody indicates that type 1 IP_3R solely functions in IP_3-induced Ca^{2+} release in mouse and hamster eggs at fertilization.

Immunoblotting experiment showed that IP_3R-1 was predominantly expressed among three different types of IP_3Rs in mouse eggs (Figure 1). Since I could not detect the immunoreactivity of IP_3R-2, I did the Western blot analysis using lysate from 1000 eggs and using polyclonal antibody to rat IP_3R-2 (data not shown). However, I could not detect the specific immunoreactive band of type 2 IP_3R.

Before analyzing the intrinsic properties of functional Ca^{2+} store, it is worth examining the localizations of IP_3Rs and Ca^{2+}-ATPase in the egg. I tried to immunolocalize the SERCA2b (isoform of Ca^{2+}-ATPase that shown to be expressed uniformly in all cell types) in the eggs and to examine the co-localization of these Ca^{2+} pumps and the IP_3R. Using a monoclonal antibody to SERCA2b, I performed the Western blot experiment, however, could not detect the specific immunoreactivity (data not shown). Preliminary observation from Western blot analysis using another monoclonal antibody suggested that another isoform of Ca^{2+}-ATPase SERCA3 may be expressed in mature mouse eggs (data not shown). It will be informative to further study the expression of Ca^{2+}-ATPase in the mouse egg.

On the other hand, using specific antibody to IP_3R-1; 4C11, I immunolocalized the IP_3Rs in eggs. This experiment showed that these IP_3R-1s were localized in the cortex as clusters (Figure 2). Although there is a fine endoplasmic reticulum (ER) network in the interior of the mouse egg (Mehlmann *et al.*, 1995), IP_3R-1 was not detected in the interior of the egg. It is likely that some IP_3Rs are present throughout the interior of eggs, since Ca^{2+} wave propagation through the inner cytoplasm of hamster eggs is dependent on IP_3Rs (Miyazaki *et al.*, 1992b; Shiraishi *et al.*, 1995).

However, the Ca^{2+} wave at fertilization in the mouse egg has not been examined carefully. Recently it has been reported that sperm-induced Ca^{2+} waves in the human egg propagate through the cortical region before moving through the interior cytoplasm (Tesarik *et al.*, 1995), suggesting some segregation of Ca^{2+} stores similar to those observed in the mouse egg.

5. Figures

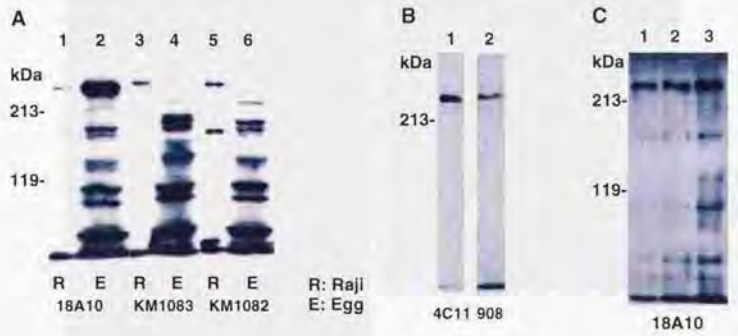

Fig. 1. Westernblotting of IP_3 receptors in mouse eggs.

Type 1 IP_3 receptor (IP_3R-1) is dominantly expressed in mature mouse eggs. Lysate from ZP-free eggs was electrophoresed under reducing condition and probed with antibodies specific for each IP_3R subtypes (18A10 and 4C11 for IP_3R-1, KM1083 for IP_3R-2 and KM1082 for IP_3R-3, 908 for all subtypes). **A**, total protein from 500 eggs (*lane* 2, 4 and 6) and membrane fraction from Raji cells (*lane* 1, 3 and 5) were subjected to SDS-PAGE followed by immunoblotting with antibodies (18A10; *lane* 1 and 2, KM1083; *lane* 3 and 4, KM1082; *lane* 5 and 6). **B**, lysate from 200 eggs was probed with hybridoma culture supernatant of 4C11 (*lane* 1) and antibody 908 (2 μg/ml; *lane* 2). Antibody 908 was affinity purified using Ampure PA column (Amersham) followed by antigen peptide-conjugated cellulofine. **C**, lysate from approximately 25 (*lane* 1), 50 (*lane* 2) and 75 (*lane* 3) ZP-free eggs were electrophoresed and probed with 18A10.

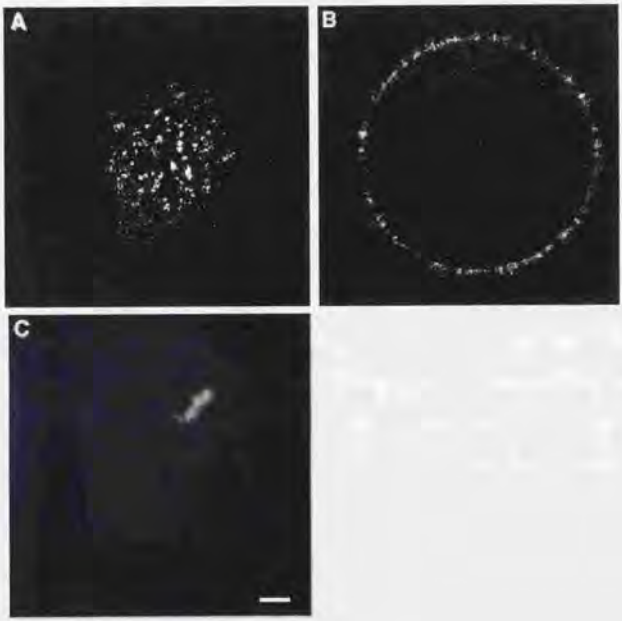

Fig. 2. Confocal sections of type 1 IP_3 receptors in eggs.

Immunofluorescently labeled type 1 IP_3 receptors localized as clusters at the cortex of mature eggs. Fixed eggs were stained with 4C11 antibody against IP_3R-1 and observed with laser-scanning confocal microscope. **A**, typical image of FITC-fluorescence from an optical section (approximately 5 μm) viewed at the surface of an egg (n = 4). **B**, image of an equatorial section of the same egg as in A. **C**, flurorescent image of Hoechst 33342 staining of the same egg as in A and B. Scale bar represents 10 μm.

Chapter II

Ca^{2+} oscillations in mouse egg

1. Introduction

A long series of transient elevations of $[Ca^{2+}]_i$ occur after fertilization of the mouse egg. The precise function and consequences of these Ca^{2+} oscillations remain as unknown in mammalian eggs as they do in many somatic cell types that undergo prolonged Ca^{2+} oscillations (Berridge and Galione, 1988; Miyazaki, 1991; Sun *et al.*, 1992; Kline and Kline, 1992a). In mammalian eggs, it appears that the temporal oscillations of $[Ca^{2+}]_i$ is based primary on the modulated release and re-uptake of Ca^{2+} from intracellular stores (Igusa and Miyazaki, 1983; Kline and Kline, 1992a). On the other hand, undergoing of the repetitive Ca^{2+} oscillations must have a feature in the necessity to move Ca^{2+} between the cytosol and storage sites by sequestration, a process that is principally, perhaps exclusively, attributable to the action of Ca^{2+}-ATPase (SERCA pumps) (Missiaen *et al.*, 1991).

Accordingly, inhibition of Ca^{2+}-ATPase and Ca^{2+} influx pathway should be disruptive to induced oscillations. Effect of Ca^{2+}-ATPase inhibitor thapsigargin on sperm-induced Ca^{2+} oscillation has been observed (Kline and Kline, 1992b). However, they have not examined the effect of thapsigargin on thimerosal-induced oscillation and have not examined the effect of another Ca^{2+}-ATPase inhibitor. Moreover, the aspect of Ca^{2+} influx during Ca^{2+} oscillations is not well examined.

To investigate the mechanisms of Ca^{2+} oscillations, it was necessary to induce the Ca^{2+} oscillation effectively in individual eggs. Therefore, I

used a sulfhydryl-reagent, thimerosal that mimic the large and persistent Ca^{2+} oscillations seen at fertilization in eggs. Thus, with this drug which can effectively induce Ca^{2+} oscillations, it is possible to eliminate any factor from the sperm that affects the Ca^{2+} signaling in mouse egg.

In this chapter, in order to investigate the role of Ca^{2+}-ATPase and Ca^{2+} influx mechanism at Ca^{2+} oscillation in mature mouse eggs, I used two chemically unrelated Ca^{2+}-ATPase inhibitors thapsigargin and 2,5-di-(*tert*-butyl)-1,4-hydroquinone (BHQ) and an antagonist for capacitative calcium entry SK&F 96365. With these tools, I pharmacologically examined the effect of Ca^{2+}-ATPase inhibitors and an antagonist for capacitative calcium entry on Ca^{2+} stores and Ca^{2+} oscillations induced by sperm and thimerosal.

2. Materials and methods

Measurement of intracellular free calcium concentrations

ZP-free eggs were loaded with fura-2 AM (1 μM; Molecular Probes) for 15 to 20 min in TYH medium at 37 °C and washed extensively with the medium. Eggs were then transferred to 10 mM HEPES (pH 7.4) containing TYH medium without BSA so the eggs would more readily adhere to glass-bottomed petri dishes (MatTek Corp., MA, U.S.A.) precoated with poly-L-lysine and placed on the stage heated at 34-36 °C of a Olympus IX70 inverted microscope for imaging.

Intracellular free divalent cation activity was imaged through a 20 x (Olympus UApo/340, NA 0.75) objective lens and silicone-intensified target (SIT) camera (C2400-08; Hamamatsu Photonics, Hamamatsu, Japan), by calculating the ratio of fura-2 fluorescence at 510 nm, excited by UV light passed through a neutral density filter (1.2 % transmission) alternately at 340 nm and 380 nm from Xenon arc lamp (75W). Excitation wavelengths were alternately irradiated through interference filters for 340 nm (band width, 25 nm) and 380 nm (band width, 25 nm) respectively and recorded the fluorescence intensity at 510 nm (band width, 25 nm) at dual excitation wavelength of 340 nm and 380 nm. In most cases, data were sampled at 5 seconds interval, but for long period of analysis, sampling were done every 10 or 20 seconds. Data sets were stored on the hard disk of the computer as digital images, and images from the square area (approximately 10 x 10 μm) at the center of eggs were processed to calculate the ratio of the fluorescence (R = F340/F380). A calibration curve between R and $[Ca^{2+}]_i$ was obtained by measuring Rs of Ca^{2+}-EGTA buffer solution (Molecular Probes) containing 2 μM fura-2 at 34.5 °C under same optical settings used for measurements. Because

of the various assumptions and reliance on external calibration buffers, the calculated $[Ca^{2+}]_i$ in cells should be considered approximations rather than absolute values, and ratio values are generally presented rather than $[Ca^{2+}]_i$. Calibration curve between ratio (R = F340/F380) and Ca^{2+} concentration was linear, in the ratio range of 0.6 to 3. A fluorescence ratio of 0.8 corresponded to a $[Ca^{2+}]_i$ of 100 nM, a ratio of 1.2 was 150 nM and ratio of 2.8 was 1.35 µM. Change of the fluorescence ratio (expressed as ΔR) was calculated by subtracting the basal ratio from maximal peak ratio (R_{peak}). Statistical comparisons were made using the Student's t test. All procedures from image acquisition through $[Ca^{2+}]_i$ calculation were accomplished with an image processor (Argus 50, Hamamatsu Photonics).

For the recording of $[Ca^{2+}]_i$ at IVF, a small amount of sperm suspension was added to 150 or 200 µl drop of TYH medium containing the experimental eggs, under mineral oil. The final sperm concentration was 5-20 x 10^3 sperm/ml and final BSA concentration was 2-3 mg/ml. To determine whether the fura-2 loaded eggs had been fertilized, the coverslip was examined under bright field for evidence of polar body (PB) extrusion.

3. Results

3.1 Effect of Ca^{2+}-ATPase inhibitors on Ca^{2+} stores

The sesquiterpene lactone, thapsigargin (TG) and synthetic compound 2.5-di-(*tert*-butyl)-1,4-hydroquinone (BHQ) are known as selective inhibitors and have been used as a tool to interfere with Ca^{2+} store function and content (Thastrup *et al.*, 1990; Moore *et al.*, 1987). Thapsigargin inhibits the endoplasmic reticulum and sarcoplasmic reticulum Ca^{2+}-ATPase (Ca^{2+} pumps) with little effect on the plasma membrane Ca^{2+}-ATPase (Thastrup *et al.*, 1990; Lytton *et al.*, 1991; Sagara and Inesi, 1991). By preventing reuptake from leaky stores, thapsigargin elevates $[Ca^{2+}]_i$ in a variety of cell types without stimulating production of inositol polyphosphates (Jackson *et al.*, 1988; Takemura *et al.*, 1989; Law *et al.*, 1990; Ely *et al.*, 1991) and has no significant effect on protein kinase C (PKC).

Another inhibitor of intracellular Ca^{2+}-ATPase; BHQ shares the mechanism of action with thapsigargin. It is frequently used and exhibits less inhibitory potency and selectivity similar to that of cyclopiazonic acid (CPA) (Foskett and Wong, 1992; Wictome *et al.*, 1992; Mason *et al.*, 1991).

I first examined the ability of thapsigargin (TG) and BHQ to alter cytosolic $[Ca^{2+}]_i$ in mouse eggs.

3.1.1 Effect of thapsigargin and BHQ on intracellular Ca^{2+} concentrations

In the presence and absence of external Ca^{2+}, TG induced a dose-dependent rise in $[Ca^{2+}]_i$ consisting of a rapid rising and rather slow falling peak as illustrated in Figure 3. The pattern of TG-induced Ca^{2+}

release from intracellular stores, as measured by the transient rise in $[Ca^{2+}]_i$ in the absence of extracellular Ca^{2+} (*right panel* in A) was similar to that of $[Ca^{2+}]_i$ increase in the presence of external Ca^{2+} (*left panel* in A), however, the amplitude of the $[Ca^{2+}]_i$ increase was smaller compared to the increase in the presence of external Ca^{2+}. Thapsigargin induced increase in $[Ca^{2+}]_i$ in the presence of external Ca^{2+} was due to the release from intracellular store and Ca^{2+} influx from extracellular fluid. Addition of 1 μM TG in the presence of external Ca^{2+} (n = 17) to the unfertilized egg caused a transient increase in $[Ca^{2+}]_i$. Similar increases in $[Ca^{2+}]_i$ during 1 μM TG (n = 6) exposure were observed in the absence of external Ca^{2+}. At TG concentrations of 20 μM, the treatment caused a monotonic rise in $[Ca^{2+}]_i$ both in Ca^{2+}, Mg^{2+}-containing TYH medium (n = 7) and in Ca^{2+}, Mg^{2+}-free TRS medium containing 1 mM EGTA (n = 5). In the range studied, addition of 0.5-10 μM TG caused dose-dependent increase in $[Ca^{2+}]_i$ (*closed square* in Figure 3B) in the absence of external Ca^{2+}. Since treatment of eggs with TG concentration of 0.1 to 0.5 μM caused oscillatory responses, values from the measurement at those range of TG concentration were not plotted in the Figure 3B. In the absence of external Ca^{2+} (Ca^{2+}, Mg^{2+}-free TRS medium containing 1 mM EGTA), a maximal increase in $[Ca^{2+}]_i$ were obtained between the range of 5 μM to 100 μM (*closed square* in Figure 3B). Thus, TG concentration of 20 μM was used for further experiments.

Similar analysis of the effect of BHQ on $[Ca^{2+}]_i$ was performed and representative traces of eggs treated with BHQ are illustrated in Figure 4A. The release of Ca^{2+} induced by 5 μM BHQ (n = 7) was similar with the release induced by TG. Treatment of eggs with 20 μM BHQ showed two typical type of release. Among fourteen eggs examined, six eggs showed a monotonic type of rise as those seen in eggs treated with 20 μM BHQ (6 out of 14 eggs). Other eggs showed rather fast rising and had fast

falling and followed by slow decline in $[Ca^{2+}]_i$ to the basal level (8 out of 14 eggs). However, treatment of eggs with 20 μM BHQ did not induce maximal Ca^{2+} release at the concentration that can induce maximal release by TG. The dose dependence of the increase in $[Ca^{2+}]_i$ induced by BHQ in the presence and absence of external Ca^{2+} is summarized in Table 1. In the range studied, the Ca^{2+} released by BHQ increased with the concentration of the inhibitor, reaching a maximum of amplitude around 100 μM (ΔR = 1.35 ± 0.20; n = 28) in the absence of extracellular Ca^{2+} (Ca^{2+}, Mg^{2+}-free TRS medium containing 1 mM EGTA). Similar increases were observed with the eggs treated with 100 μM BHQ in Ca^{2+}, Mg^{2+}-free TRS medium (n = 22; for example Figure 7B, E and H).

Therefore, I routinely used TG and BHQ at the concentration of 20 μM and 100 μM, respectively, to insure maximal Ca^{2+} release from the intracellular Ca^{2+} stores and deplete the stores for further experiment.

3.1.2 Effect of thapsigargin and BHQ on the Ca^{2+} stores

Although it is apparent that thapsigargin and BHQ release comparable amounts of Ca^{2+} from the intracellular Ca^{2+} store, it is not clear whether the same store is affected. It is possible that these two inhibitors might release Ca^{2+} from different stores. To examine this possibility, I next investigated the degree of overlap between the stores by addition of two inhibitors sequentially to the egg.

While the addition of 20 μM TG resulted in a transient rise in $[Ca^{2+}]_i$, subsequent addition of 100 μM BHQ was found to be no effect (Figure 5A, n = 8). When the order of treatment was reversed, first addition of BHQ induced a marked transient increase in $[Ca^{2+}]_i$, with the secondary addition of TG having no detectable increase in $[Ca^{2+}]_i$ (Figure 5B, n = 11). These findings suggest that the Ca^{2+} stores depleted by both

inhibitors overlap extensively. Moreover, eggs treated with both TG and BHQ showed additional Ca^{2+} release from the intracellular stores when treated with Ca^{2+} ionophore indicating the presence of another TG- and BHQ-resistant or insensitive Ca^{2+} storage compartment(s) in mouse egg.

It has been shown that mouse eggs are caffeine-insensitive cells (Kline and Kline, 1994). I next examined the involvement of caffeine-sensitive Ca^{2+} store. I investigated whether caffeine could mobilize $[Ca^{2+}]_i$ by activating the ryanodine receptor (RyR) in eggs. Consistent with the result from Kline et. al., application of 10 mM caffeine (Figure 6A, n = 8) did not result in increase of $[Ca^{2+}]_i$, thereby indicating no apparent property of caffeine-sensitive Ca^{2+} release in mature mouse eggs.

3.2 Effect of Ca^{2+}-ATPase inhibitors on Ca^{2+} influx

In many cell types, increase in Ca^{2+} permeability of the plasma membrane is triggered by the depletion of critical intracellular Ca^{2+} storage compartment. This unknown mechanism is called "Capacitative Calcium Entry (CCE)" which was proposed by Putney (Putney, 1986; Putney, 1990). This hypothesis is based largely on the effect of thapsigargin. Emptying the thapsigargin-sensitive store promotes Ca^{2+} influx (Ca^{2+} entry), in many cells (Thastrup *et al.*, 1990; Takemura *et al.*, 1989; Law *et al.*, 1990; Mason *et al.*, 1991), but not in all cells (Jackson *et al.*, 1988; Llopis *et al.*, 1991), without change in the level of inositol phosphates (Jackson *et al.*, 1988). On the other hand, depletion of the intracellular stores by high concentration of BHQ, failed to induce Ca^{2+} influx in other cell types (Kass *et al.*, 1989; Missiaen *et al.*, 1992; Foskett and Wong, 1992).

It has been suggested that the phase of thapsigargin-induced elevation of $[Ca^{2+}]_i$ which is dependent on extracellular Ca^{2+}, is voltage-insensitive,

and can be blocked by inorganic ions such as Ni^{2+} or by a new channel blocker specific for this site, SK&F 96365 (Merritt *et al.*, 1990; Demaurex *et al.*, 1992). I next investigated the effect of Ca^{2+}-ATPase inhibitors on divalent cation entry across the plasma membrane and further tested for the ability of the antagonist for capacitative calcium entry SK&F 96365 to inhibit the Ca^{2+} influx pathway.

3.2.1 Effect of thapsigargin and BHQ on divalent cation entry

Eggs were treated with TG (20 μM) or BHQ (100 μM) in Ca^{2+}, Mg^{2+}-free TRS medium to deplete the stores and three different divalent cations were added to the extracellular medium. As shown in Figure 7A and D, addition of TG activated an influx pathway for divalent cations across the plasma membrane; a second surge in $[Ca^{2+}]_i$ was observed when 4.6 mM $CaCl_2$ was added to eggs previously treated with 20 μM TG in Ca^{2+}, Mg^{2+}-free TRS medium (Figure 7A, n = 5). There was little change in $[Ca^{2+}]_i$ over a 60 min period when 4.6 mM $CaCl_2$ was added to control eggs not previously treated with TG (Figure 7C, n = 14). Among them, two eggs showed spontaneous transients (data not shown). A larger, immediate increase in $[Ca^{2+}]_i$ occured with addition of 4.6 mM $SrCl_2$ after treatment with TG (Figure 7D, n = 7). Addition of $SrCl_2$ caused repetitive Ca^{2+} transient in eggs (Figure 7F, n = 4). This Ca^{2+} oscillation continued for more than an hour (data not shown). Addition of 4.6 mM $MgCl_2$ with prior TG treatment caused no increase in $[Ca^{2+}]_i$ (Figure 7G, n = 6) nor the treatment of eggs with 4.6 mM $MgCl_2$ alone had no effect on the $[Ca^{2+}]_i$ (Figure 7I, n = 14). In contrast, the effect of BHQ on the Ca^{2+} influx differed markedly from that of thapsigargin. Addition of three different divalent cations; $CaCl_2$ (Figure 7B, n = 9), $SrCl_2$ (Figure 7E, n = 12) and $MgCl_2$ (Figure 7H, n = 6) to eggs previously treated with

100 μM BHQ in Ca^{2+}, Mg^{2+}-free TRS medium either failed to induce Ca^{2+} influx across the plasma membrane. Similar inhibitory effect of BHQ on Ca^{2+} influx across the plasma membrane has been reported in other cell types (Kass *et al.*, 1989; Mason *et al.*, 1991; Foskett and Wong, 1992).

3.2.2 Effect of SK&F 96365 on thapsigargin-induced Ca^{2+} influx

Similar with the experiment in Figure 7, addition of $CaCl_2$ to the eggs previously treated with 20 μM TG in Ca^{2+}, Mg^{2+}-free TRS medium containing 1 mM EGTA resulted in Ca^{2+} influx across the plasma membrane (Figure 8A, n = 9). In contrast to TG, BHQ treated eggs did not cause Ca^{2+} influx (Figure 8B, n = 5). As shown in Figure 8C, Ca^{2+} influx due to depletion of Ca^{2+} stores by thapsigargin was inhibited by pretreatment with 50 μM SK&F 96365 in 1 mM EGTA containing Ca^{2+}, Mg^{2+}-free TRS medium (n = 7) and in Ca^{2+}, Mg^{2+}-free TRS medium without EGTA (n = 21; data not shown). SK&F 96365 treatment of eggs previously treated with 100 μM BHQ had no effect on $[Ca^{2+}]_i$ when 4.6 mM $CaCl_2$ was added to the egg (n = 10, data not shown). Addition of 20 μM SK&F 96365 also inhibited Ca^{2+} influx in Ca^{2+}, Mg^{2+}-free TRS medium containing 1 mM EGTA (n = 1; data not shown).

These phenomena, shown above, are generally accepted as evidence of CCE. These results suggest that intrinsic mechanism that coupled with the depletion of the thapsigargin (and BHQ)-sensitive Ca^{2+} store and activation of Ca^{2+} influx is present in the mature mouse eggs and may work during Ca^{2+} oscillations at fertilization.

3.3 Ca^{2+} oscillations induced by sperm and thimerosal

Interaction between mouse egg and sperm at fertilization triggers a large and long increase in $[Ca^{2+}]_i$ in the egg cytoplasm which is followed by repetitive Ca^{2+} transients. At fertilization of mouse eggs, the pattern of Ca^{2+} transients varied considerably between eggs and strains of mice and there is even some variabillity in the frequency of oscillations among individual mouse eggs under similar conditions (Kline and Kline, 1992a; Swann, 1992).

On the other hand, a sulfhydryl-reagent, thimerosal, mimics the large and persistent Ca^{2+} oscillations seen at fertilization most successfully, in both hamster and mouse eggs (Miyazaki *et al.*, 1992a; Swann, 1991; Swann, 1992). With this drug, it is possible to induce the Ca^{2+} oscillations reproduciblly in mouse egg.

It has been shown that the sulfhydryl-oxidizing reagent thimerosal (ethylmercurithiosalicylate) causes $[Ca^{2+}]_i$ increases in platelets and leukocytes (Hecker *et al.*, 1989; Hatzelmann *et al.*, 1990). These observations suggested that sulfhydryl groups are involved in a Ca^{2+} release mechanism. Swann et al. showed that thimerosal causes a series of Ca^{2+}-dependent hyperpolarizing responses (HRs) in unfertilized hamster eggs (Swann, 1991). The series of Ca^{2+} transients induced by thimerosal are observed in eggs of a number of mammalian species (Fissore *et al.*, 1992; Kline and Kline, 1994; Miyazaki *et al.*, 1992a). Recently, thimerosal-induced Ca^{2+} release has been reported for immature mouse oocytes and mature mouse eggs (Kline and Kline, 1994). Furthermore, Miyazaki et al. (Miyazaki *et al.*, 1992a) reported that the monoclonal antibody to the IP_3R blocked Ca^{2+} oscillations induced by thimerosal in the hamster egg, indicating that thimerosal causes Ca^{2+} oscillations by an effect dependent on the IP_3R. Treatment of unfertilized mammalian eggs with thimerosal is the simplest and most effective way of artificially causing the Ca^{2+} oscillations.

Thimerosal mimics the pattern of the Ca^{2+} oscillations induced by sperm, however, the signal that generates the Ca^{2+} release may be little different. Thimerosal probably acts by oxidizing-sulfhydryl groups, a process that should be reversed by reducing reagent dithiothreitol (DTT) (Cheek *et al.*, 1993). It is suggested that the thimerosal induces Ca^{2+} without affecting the inositol-phosphate level (Bootman *et al.*, 1992). Recently, a role for PLC at fertilization has been examined using U73122 in intact mouse eggs (Dupont *et al.*, 1996). U73122 exhibited an inhibitory action on acetylcholine- and sperm-induced Ca^{2+} oscillations, and did not inhibit TMS-induced Ca^{2+} oscillations. Results from the experiment using the PLC inhibitor in my experiment (data not shown) and the report from Dupont et al. indicated that in contrast to sperm, thimerosal-induced $[Ca^{2+}]_i$ release may not be a consequence of IP_3 production. The consensus of the action of thimerosal is that the oxidative state of protein thiol groups present in the IP_3R itself is able to influence IICR at the basal concentration level of IP_3 in the cytosol.

3.3.1 Ca^{2+} oscillations induced by sperm

Eggs from ICR mouse were loaded with fura-2 and recording of $[Ca^{2+}]_i$ was started after addition of the sperm suspension into the drop of medium. Representative Ca^{2+} responses of eggs to sperm are illustrated in Figure 9. Repetitive Ca^{2+} transients induced by sperm continued for more than two hours. Following the insemination, the initiation of Ca^{2+} transients in the first egg began after a delay of about 15-40 minutes and the first transient was broader and had a larger amplitude than the subsequent transients as has been described by others (Kline and Kline, 1992a; Swann, 1992). The subsequent pattern of Ca^{2+} transients varied considerably between eggs and strains of mice and, as shown in Figure 9,

there was even some variabillity in the frequency of oscillations among individual mouse eggs under similar conditions. Variability of transients were seen with the eggs from other strain of mice; B6C3F1 (n = 20, two measurements with fura-2, data not shown) and with another measurement using calcium green-1 as a calcium indicator (n = 29, four measurements with eggs from ICR mouse, data not shown). In most experiments, some eggs remained unfertilized; the Ca^{2+} levels in these eggs served as controls for those in fertilized eggs. In most eggs, there was a gradual reduction in amplitude of the each transients with time, as recorded in previous experiments on mouse (Cuthbertson, 1983) and hamster (Igusa and Miyazaki, 1983) eggs. We have observed trains of Ca^{2+} transients up to almost three hours (Figure 9). Such Ca^{2+} transients can continue for as long as four hours after fertilization (Kline and Kline, 1992b; Jones *et al.*, 1995).

3.3.2 Ca^{2+} oscillations induced by thimerosal

Addition of thimerosal (TMS) to unfertilized mouse egg produced a series of Ca^{2+} transients which also usually began with a much broader peak, as observed for sperm-induced oscillations. A characteristic feature of each transients is the gradual pacemaker rise in Ca^{2+} that precedes the rapid rising phase and subsequently, the $[Ca^{2+}]_i$ rise declined, associated with the first slow phase and the second rapid phase. The threshold for the stimulatory action of TMS was around 10 μM (Figure 10A, n = 6). Among six eggs, three eggs showed no change in $[Ca^{2+}]_i$ for 50 min and other three eggs showed two to three transients which had short duration of 13 to 15 min after the treatment. Application of 250 μM TMS produced repetitive Ca^{2+} transients in all eggs examined in these experiments. Treatment with 250 μM TMS in normal Ca^{2+}-containing

medium caused a gradual increase in $[Ca^{2+}]_i$ began 2 to 3 min later and oscillations usually lasted for an hour (Figure 10B, n = 12). With time, amplitude of each transient gradually declined and freqeuncy of oscillation became higher. Further raising the concentration to 500 μM (n = 12; data not shown), 1 mM (n = 13; data not shown), 5 mM (Figure 10C, n = 12) and 20 mM (n = 12; data not shown) showed no oscillations but resulted in sustained increase in $[Ca^{2+}]_i$ for over 30 min. I used the TMS concentration of 250 μM for further experiment which has a large amplitude and long lasting Ca^{2+} oscillations.

I next investigated whether TMS-induced Ca^{2+} oscillations depend on extracellular Ca^{2+}. Eggs treated with 120 μM (n = 10; data not shown) and 250 μM TMS (Figure 10D, n = 7) in Ca^{2+}, Mg^{2+}-free TRS medium showed a series of Ca^{2+} transients. First Ca^{2+} transient was broad as those seen in Ca^{2+}-containing TYH medium, however the amplitude of Ca^{2+} transient and basal $[Ca^{2+}]_i$ level slightly declined with time. When eggs were treated with 250 μM TMS, Ca^{2+} transients disappeared around 40 to 60 minutes after the treatment. Similar pattern of rise in $[Ca^{2+}]_i$ were observed in Ca^{2+}, Mg^{2+}-free TYH medium containing 5 mM EGTA (n = 7, data not shown) and in Ca^{2+}, Mg^{2+}-free TRS medium containing 1 mM EGTA (n = 5, data not shown). Large proportion of Ca^{2+} stores was depleted by TMS-induced Ca^{2+} oscillations in Ca^{2+}, Mg^{2+}-free TRS medium. As shown in Figure 11B (n = 27), treatment of Ca^{2+} ionophore 4-Br A23187 (5 μM) after TMS-induced Ca^{2+} transients had stopped, additional Ca^{2+} was released from intracellular Ca^{2+} stores. Magnitude of the additional release of Ca^{2+} from the eggs treated with TMS was always small compared to that of eggs treated with Ca^{2+} ionophore alone (Figure 11A, n = 25).

Thimerosal induced Ca^{2+} transients in the absence of extracellular Ca^{2+} (Figure 10D), indicating that TMS-induced oscillations in mouse egg

consist of repetitive Ca^{2+} release from intracellular stores. The difference between the oscillations induced by TMS in Ca^{2+}-containing medium and in Ca^{2+}, Mg^{2+}-free medium indicates the requirement of extracellular Ca^{2+} for the maintenance of the amplitude and the frequency of oscillations.

3.4 Effect of SK&F 96365 on Ca^{2+} oscillations induced by thimerosal

Thimerosal-induced Ca^{2+} oscillations in Ca^{2+}, Mg^{2+}-free medium showed no marked acceleration of frequency as compared to the oscillations in Ca^{2+}-containing medium (Figure 10D). This result indicates that the frequency of oscillation is dependent on the extracellular Ca^{2+}. As I have shown previously, SK&F 96365 inhibited the TG-induced Ca^{2+} influx across the plasma membrane (Figure 8C). It is probable that SK&F 96365 will inhibit the Ca^{2+} influx during the Ca^{2+} oscillations. Therefore, I investigated the effect of this inhibitor on Ca^{2+} oscillations induced by thimerosal in the presence of extracellular Ca^{2+}.

Various concentration of SK&F 96365 was added to the eggs showing oscillations induced by thimerosal in normal Ca^{2+}-containing TYH medium. Period between transients (indicated as "Interval of transients" in *y-axis*) were measured between the peak of the each transient and plotted against the number of transients observed during 1 h of measurement. Figure 12A (*left panel*) shows the representative eggs (from the eggs shown in the *right panels*) treated with indicated concentration of SK&F 96365. As shown in the right panel, period between the transients became longer with increasing dose of SK&F 96365 (10 μM; n = 24, 20 μM; n = 23, 50 μM; n = 51). Eggs not treated with the antagonist showed the acceleration of the frequency, (Figure

12B, n = 12). However, eggs treated with 50 μM SK&F 96365 resulted in marked delay of the onset of following transients (Figure 12A, n = 10).

These results suggest that, at least in part, Ca^{2+} influx from extracellular fluid regulates the frequency of oscillation, and that this influx pathway consist of mechanism sensitive to SK&F 96365.

3.5 Effect of Ca^{2+}-ATPase inhibitors on Ca^{2+} oscillations

As previously shown in Figure 10D and 11B, thimerosal induced the persistent Ca^{2+} oscillations in the absence of extracellular Ca^{2+}, indicating that significant amount of Ca^{2+} is taken up by Ca^{2+}-ATPase into intracellular Ca^{2+} store. Inhibiting re-uptake of Ca^{2+} into the stores may have severe effect on Ca^{2+} oscillations. Therefore, I examined the effect of Ca^{2+}-ATPase inhibitors on Ca^{2+} oscillations induced by sperm and thimerosal.

3.5.1 Effect of Ca^{2+}-ATPase inhibitors on Ca^{2+} oscillations induced by thimerosal

The effect of Ca^{2+}-ATPase inhibitors TG and BHQ on TMS-induced Ca^{2+} oscillations were investigated. As previously shown in Figure 10B, addition of TMS to unfertilized eggs produced an oscillation which usually began with a much broader transient than the subsequent transients and repetitive Ca^{2+} transients with high frequency. Figure 13 shows the effect of TG on TMS-induced oscillations. Prior treatment of eggs with 20 μM TG caused a monotonic increase in $[Ca^{2+}]_i$ as shown previously, subsequently, addition of 250 μM TMS to the eggs resulted in oscillations (*upper trace* in Figure 13A, n = 18). However, the first transient appeared relatively small in amplitude and short in duration

(Ratio at the peak of the transient: $R_{peak} = 2.24 \pm 0.24$, duration at the point of half maximal: $T_{1/2} = 88 \pm 10$ sec; n = 9) as compared to the amplitude of first transient in same batch of the eggs not previously treated with TG ($R_{peak} = 2.98 \pm 0.22$, $T_{1/2} = 165 \pm 26$ sec; n = 8) ($p < 0.001$). As shown in Figure 13A (*lower trace*), raising the TG concentration to 50 μM (n = 25) markedly suppressed the frequency of the oscillation as compared to the eggs treated with 20 μM TG. Addition of 20 μM (*upper panel*, n = 19) and 50 μM (*lower panel*, n = 22) TG after 3 to 4 (approximately 15 min after treatment) transients induced by TMS in TYH medium (Figure 13C) dose-dependently decreased the frequency of subsequent oscillations as compared to the eggs treated with 0.2 % DMSO (Figure 13E, n = 7; the same concentration of DMSO with 20 μM TG). To exclude the contribution of Ca^{2+} influx activated by TG, same examination was done in the absence of extracellular Ca^{2+}. Prior treatment of eggs with 20 μM TG in Ca^{2+}, Mg^{2+}-free TRS medium containing 1 mM EGTA did not completely inhibit Ca^{2+} oscillations induced by TMS (*upper trace* in Figure 13B, n = 17). However, similar with the result in Figure 13A, the duration of first transient was suppressed. Same effect of TG was seen with the eggs treated in Ca^{2+}, Mg^{2+}-free TRS medium (n = 14, data not shown). Raising the TG concentration to 50 μM (*lower trace* in Figure 13B, n = 13) resulted in marked inhibition of subsequent transients. Among thirteen eggs examined, eleven eggs showed one or two transients and other two eggs showed no transient at all. Addition of 20 μM and 50 μM TG after 3 to 4 transients induced by TMS in Ca^{2+}, Mg^{2+}-free TRS medium had little inhibitory effect on the frequency of subsequent oscillations (Figure 13D, n = 8 for 20 μM and n = 5 for 50 μM respectively).

Another inhibitor BHQ exhibited almost complete inhibition of oscillations when BHQ was added after few transients had started in

response to TMS. Inhibition of subsequent transients was observed with eggs treated with 100 μM BHQ in normal Ca^{2+}-containing medium (Figure 14C, n = 16) and in Ca^{2+}, Mg^{2+}-free TRS medium (Figure 14D, n = 21). BHQ treatment produced a rapid increase in $[Ca^{2+}]_i$, subsequently transients ceased. Similar inhibitory effect was observed with the eggs treated with 200 μM BHQ in Ca^{2+}, Mg^{2+}-free TRS medium containing 1 mM EGTA (n = 20; data not shown). Induction of repetitive transients by TMS after pretreatment with 100 μM BHQ (*upper trace* in Figure 14A, n = 22) in TYH medium resulted in low frequency oscillations which had slow rising and falling peaks. Raising the concentration to 200 μM BHQ (*lower trace* in Figure 14A, n = 17) showed disruptive effect on the oscillations. Most of the eggs (15 out of 17) showed only one or two transients. Similar inhibitory effects were observed with the eggs treated with 100 μM (*upper trace* in Figure 14B, n = 13) and 200 μM (*lower trace* in Figure 14B, n = 14) in Ca^{2+}, Mg^{2+}-free TRS medium containing 1 mM EGTA and in Ca^{2+}, Mg^{2+}-free TRS medium (n = 16; data not shown).

Thapsigargin and BHQ both showed inhibitory effect on the Ca^{2+} oscillation induced by thimerosal in the presence and absence of extracellular Ca^{2+}. These results indicate that in mature mouse egg, Ca^{2+} pump sensitive to both inhibitors exists and functions during Ca^{2+} oscillation induced by thimerosal.

3.5.2 Effect of Ca^{2+}-ATPase inhibitors on Ca^{2+} oscillations induced by sperm

I next carried out the same experiment with sperm-induced Ca^{2+} oscillation. Eggs were treated with TG or BHQ after fertilization. When TG was added after two transients have occured, TG treatment produced

an increase in $[Ca^{2+}]_i$ (Figure 15A). However, the transient increase in $[Ca^{2+}]_i$ immediately following TG addition was short in duration as compared to that of increase normally produced by TG alone. Treatment of eggs with 20 μM (*left trace* in Figure 15A, n = 6) and 50 μM TG (*right trace* in Figure 15A, n = 4) suppressed the subsequent Ca^{2+} transients induced by sperm. Among ten eggs which were treated with high concentration (20 μM and 50 μM, n = 10) of TG, three (2 for 20 μM and 1 for 50 μM) eggs showed only one transient immediately after the treatment and no subsequent transient was observed throughout the measurement (*left trace* in Figure 15A). An egg treated with 50 μM resulted in two transients which had high frequency and showed no subsequent transients (*right trace* in Figure 15A). Other six eggs (4 for 20 μM and 2 for 50 μM) showed one transient around 30 min after the treatment and most eggs (5 out of 6 eggs) had a tendency for base line to drift upwards. Although long exposure of eggs to high concentration of TG caused damage to the eggs, TG treated eggs which appeared normal showed suppression of Ca^{2+} oscillation.

Treatment of eggs with 100 μM BHQ resulted in inhibition of the subsequent transients in all eggs examined (Figure 15B, n = 7). Two types of response were observed. In one case, as shown in Figure 15B (*left trace*), BHQ induced three to four transients immediately after the treatment of the inhibitor and subsequent transients disappeared (2 out of 7 eggs). These eggs showed similar transients as observed with the eggs treated with 50 μM TG in right panel in Figure 15A. The following transients were usually reduced in amplitude and, in these eggs, BHQ temporarily shortened the period between transients. In other case (5 out of 7 eggs), BHQ induced one large increase and one small transient and no subsequent transients were observed throughout the measurement (*right trace* in Figure 15B).

4. Discussion

4.1 Effect of Ca^{2+}-ATPase inhibitors on intracellular Ca^{2+} concentrations in eggs

It has been suggested that there are roughly two types of response in cells treated with high concentrations of thapsigargin. There are the release from stores is then followed either by return of $[Ca^{2+}]_i$ to the prestimulatory levels or by maintained elevated plateau reflecting an increased Ca^{2+} influx through plasma membrane channels. The ability of thapsigargin and BHQ to alter cytosolic $[Ca^{2+}]_i$ in mouse eggs was examined. Both in the presence and absence of external Ca^{2+}, thapsigargin induced a monotonic dose-dependent rise in $[Ca^{2+}]_i$, as illustrated in Figure 3A and did not appeared to be a sustained type of increase in $[Ca^{2+}]_i$. This may be due to the action of plasma membrane Ca^{2+}-ATPase (PMCA) pumping Ca^{2+} out of the egg cytosol. Thapsigargin induced increase in $[Ca^{2+}]_i$ in the presence of external Ca^{2+} was due to the release from intracellular store and Ca^{2+} influx from extracellular fluid. Maximal Ca^{2+} release response was observed at thapsigargin concentrations of 20 μM in the absence of external Ca^{2+} (Figure 3B). I used another chemically unrelated synthetic compound BHQ as Ca^{2+}-ATPase inhibitor (Figure 4). Dose dependent rise in $[Ca^{2+}]_i$ were also seen with BHQ and concentration of 100 μM was needed to maximally induce Ca^{2+} release similar to that of thapsigargin from the intracellular stores and to deplete the store. Thastrup et al. introduced thapsigargin into widespread use and is normally effective at concentrations below 1 μM (Thastrup *et al.*, 1990). In general, to achieve measurable Ca^{2+} discharge in fura-2 loaded cells, thapsigargin should be used at concentrations ranging from 20 to 100 nM, but frequently is used at

higher concentrations to insure maximal Ca^{2+} release. In many cells, a significant mismatch exists between Ca^{2+}-ATPase inhibitor concentrations required to elicit Ca^{2+} discharge rather than the pump arrest, because of the efficiency and kinetics of cell penetration by these inhibitors. Upon inhibition of Ca^{2+}-ATPase (SERCA), BHQ required a half-maximal inhibitory concentration of about 0.4 μM for the rabbit SERCA 1a isoform (Wictome *et al.*, 1992). However, in intact lymphocytes, BHQ required a concentration of 30 μM for maximal Ca^{2+} release (Mason *et al.*, 1991). As previously observed with thapsigargin by Kline et al. in mouse eggs (Kline and Kline, 1992b), like *Xenopus* oocytes (Petersen and Berridge, 1994), mouse eggs were relatively insensitive to these inhibitors. Thus, Ca^{2+} release in eggs required higher concentrations of these reagents.

4.2 Relationships between Ca^{2+} stores in mouse eggs

It is conceivable that the different pattern of increase in $[Ca^{2+}]_i$ induced by thapsigargin and BHQ (Figure 3 and 4) in Ca^{2+}-containing medium and the fact that additional Ca^{2+} release can be induced (Figure 5) reflects the involvement of different stores. Many experiments on Ca^{2+} storage pools are performed simply by the sequential addition of multiple hormones or drugs to intact cells to determine whether Ca^{2+} discharge induced by one agent can abolish the effect of the other. I have sequentially added thapsigargin and BHQ to the eggs and showed that these two inhibitors acted upon same intracellular Ca^{2+} stores and overlapped extensively (Figure 5). Since no distinction has been found between the Ca^{2+} stores defined by the use of different Ca^{2+}-ATPase inhibitors, that is, Ca^{2+}-ATPase inhibition defines the same functional store regardless of the inhibitor used. It has been suggested that

thapsigargin depletes an IP_3-sensitive Ca^{2+} stores in some cells (Thastrup *et al.*, 1990; Takemura *et al.*, 1989; Robinson and Burgoyne, 1991), but may also affect IP_3-insensitive Ca^{2+} stores (Thastrup *et al.*, 1990; Ely *et al.*, 1991; Bian *et al.*, 1991). It was suggested by Kline et al. that in mouse eggs, the IP_3-sensitive store is not rapidly depleted of Ca^{2+} by inhibition of the Ca^{2+}-ATPase, since thapsigargin did not prevent the increase in $[Ca^{2+}]_i$ produced by injection of IP_3. Pretreatment of intact cells with high concentrations of thapsigargin (or of other inhibitors) most often results in the abolition of Ca^{2+} release by both agonists coupled to IP_3 generation and activators of ryanodine receptors. In a few cell types (parotid and chromaffin) (Foskett *et al.*, 1991; Robinson and Burgoyne, 1991), however, a residual agonists (or caffeine)-induced Ca^{2+} mobilization has been observed even after thapsigargin treatment. In contrast to IP_3-sensitive store, the caffeine-sensitive store is not ubiquitously expressed, and its presence is often revealed by administration to cells of high concentrations (10-20 mM) of caffeine. It has been peviously suggested that mouse egg does not respond to caffeine (Kline and Kline, 1994). I examined whether eggs used in this experiment contains caffeine-sensitive Ca^{2+} stores or not (Figure 6). Consistent with the result by Kline et al., application of caffeine to unfertilized eggs had no direct effect on $[Ca^{2+}]_i$, indicating that mouse eggs seems to be possessing no caffeine-sensitive stores. Although, eggs exposed to thapsigargin or BHQ showed additional Ca^{2+} release (Figure 5), it is clear that there is at least one thapsigargin (BHQ)-sensitive store in mouse egg. It is possible that TG- and BHQ-resistant or insensitive Ca^{2+} stores can be; mitochondrial Ca^{2+} stores, the store dischargeble only by Ca^{2+} ionophore (Bian *et al.*, 1991) and/or novel Ca^{2+} stores that releases Ca^{2+} by nicotinic-acid adenine dinucleotide phosphate (NAADP) recently found in sea urchin eggs (Chini *et al.*, 1995; Genazzani and Galione, 1996). Morever, I cannot exclude the

possibilities that Ca^{2+}-ATPase in mouse eggs has very low sensitivity to these inhibitors and/or existence of unknown Ca^{2+}-ATPase resistant to these inhibitors.

4.3 Mechanism of Ca^{2+} oscillations in mouse eggs

Ca^{2+} oscillations induced by both sperm and thimerosal in mouse egg consist of repetitive Ca^{2+} release from intracellular stores, since thimerosal induced Ca^{2+} transients in the absence of extracellular Ca^{2+} (Figure 10D) and sperm induces several transients in the absence of extracellular Ca^{2+} (Kline and Kline, 1992b). However, extracellular Ca^{2+} was required to maintain the large amplitude and duration of each transients and frequency of oscillations (Figure 10 and 12). I have successfully inhibited the site of Ca^{2+} influx pathway by using the antagonist for capacitative calcium entry SK&F 96365 (Figure 12). SK&F 96365 modulated the frequency of oscillation by inhibiting the Ca^{2+} influx pathway probably via undefined Ca^{2+} channel which is voltage-insensitive. These results indicate that influx of extracellular Ca^{2+} regulates the frequency of oscillation.

In this study, I have shown that thapsigargin and BHQ suppressed the Ca^{2+} oscillation induced by both sperm and thimerosal (Figure 13 to 15). However, thapsigargin did not completely prevent sperm-induced Ca^{2+} transients. It is quite possible that mouse egg is relatively insensitive to the inhibitor and the egg may contain thapsigargin-insensitive or -resistant store that may mobilized by sperm at fertilization as previously discussed by Kline et. al. (Kline and Kline, 1992b). Moderate inhibitory effect of thapsigargin on oscillations was observed when added after the thimerosal treatment (Figure 13C and D). It is possible that thapsigargin can no longer inhibit the Ca^{2+}-ATPase, since it has been suggested that

thimerosal has some aspect of affecting endoplasmic and sarcoplasmic Ca^{2+}-ATPase (Sayers *et al.*, 1993). Surprisingly, another structually unrelated inhibitor BHQ showed more severe effect on Ca^{2+} oscillations induced by both sperm and thimerosal in eggs (Figure 15C, D and Figure 14). Addition of BHQ after thimerosal treatment exhibited disruptive effect on subsequent transients (Figure 14C and D) In addition, sperm treated with BHQ appeared normal in contrast to the eggs treated with thapsigargin. It has been suggested that BHQ may interfere with additional aspects of Ca^{2+} signaling dynamics, or inhibition of the passive Ca^{2+} leak from internal stores (Missiaen *et al.*, 1992). Furthermore, BHQ has not been tested rigorously for its specificity in inhibition of other ion-motive ATPases. The discrimination between the effect of these inhibitors on Ca^{2+} oscillations cannot be simply explained by the effective concentration of these two inhibitors on Ca^{2+}-ATPase, since the efficiency and kinetics of cell penetration by these inhibitors are unknown. It is unlikely that the inhibitory action of BHQ on Ca^{2+} oscillations induced by thimerosal (Figure 14C) is the result of inhibiting Ca^{2+} influx from extracellular medium, since BHQ had a potency of inhibiting Ca^{2+} oscillations completely even in the absence of external Ca^{2+} (Figure 14B and D). Pharmacological approach using the inhibitors revealed that thapsigargin- (and BHQ-) sensitive Ca^{2+}-ATPase are likely to take up a considerable amount of Ca^{2+} into the intracellular store during oscillations induced by both thimerosal and sperm. Further experiments using another Ca^{2+}-ATPase inhibitor cyclopiazonic acid (CPA) may support the results obtained in this study. It is of interest to estimate what amount of the stored Ca^{2+} released during each transient and proportion of Ca^{2+} taken up by Ca^{2+}-ATPase present on the intracellular Ca^{2+} stores. It will be nicely studied if it is possible to measure the Ca^{2+} concentration in the cytosol and in the lumen simultaneously.

5. Tables & Figures

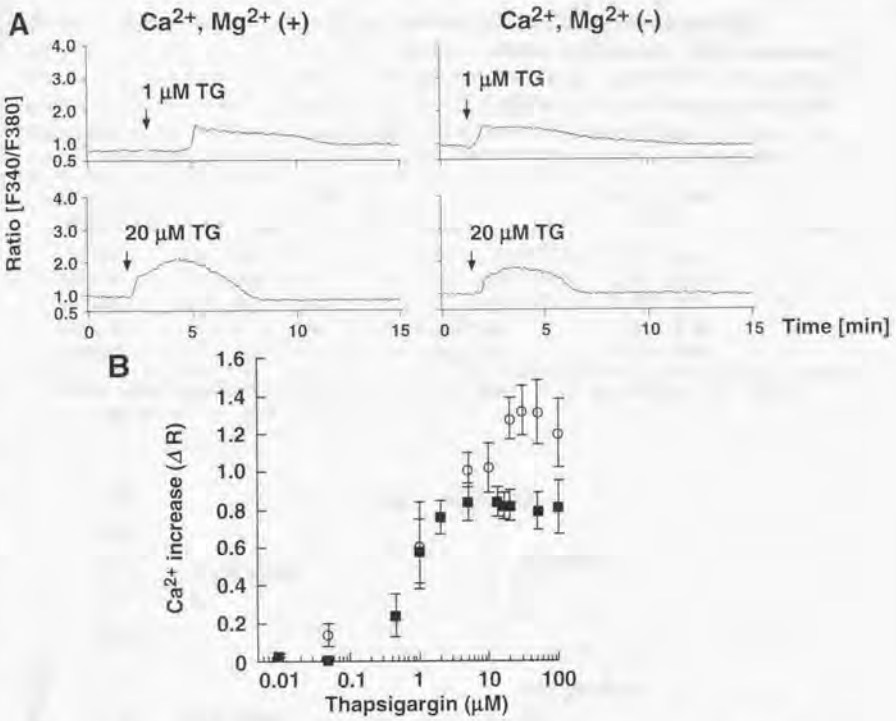

Fig. 3. The Ca^{2+}-ATPase inhibitor thapsigargin causes a transient increase in $[Ca^{2+}]_i$ in mouse eggs.

Thapsigargin (TG) dose-dependently elevates $[Ca^{2+}]_i$ from the intracellular Ca^{2+} stores in mouse egg. *Zonae pellucidae* (ZP) was removed from the egg and loaded with fura-2 before measurement as indicated under Materials and Methods. **A**, representative traces of eggs treated with indicated concentration of TG both in Ca^{2+}, Mg^{2+}-containing TYH medium (*left panel*, 1 μM; n = 17, 20 μM; n = 22) and in Ca^{2+}, Mg^{2+}-free TRS medium containing 1 mM EGTA (*right panel*, 1 μM; n = 14, 20 μM; n = 5). **B**, dose-response for $[Ca^{2+}]_i$ rise induced by TG in Ca^{2+}, Mg^{2+}-free TRS medium containing 1 mM EGTA (*closed square*) and in Ca^{2+}, Mg^{2+}-containing TYH medium (*open circle*). Change of the fluorescence ratio (ΔR; basal ratio subtracted from maximal peak ratio) obtained from measurement of 30 minutes were calculated and expressed as "Ca^{2+} increase (ΔR)". Calibration curve between ratio (R = F340/F380) and Ca^{2+} concentration was linear, in the ratio range of 0.6 to 3. Each *point* represents the mean ± S.D. (n = 3-26) of eggs from one to three batches of egg. Data are from 26 different batches of egg. Values obtained from the range of 0.1 to 0.5 μM were not plotted in the figure, since treatment of eggs with those concentration of TG caused oscillatory type of responses, but not monotonic type of responses.

Table 1. Effect of another Ca^{2+}-ATPase inhibitor BHQ on $[Ca^{2+}]_i$ in mouse eggs.

Eggs were treated with various concentrations of BHQ in normal Ca^{2+}, Mg^{2+}-containing TYH medium and in Ca^{2+}, Mg^{2+}-free TRS medium containing 1 mM EGTA. The average peak Ca^{2+} increase (ΔR) is indicated (mean ± S.D.). Change of the fluorescence ratio (ΔR; basal ratio subtracted from maximal peak ratio) obtained from measurement of 30 minutes were calculated and expressed as "Ca^{2+} increase (ΔR)". n is the number of eggs examined.

Concentration of BHQ	Medium	Ca^{2+} increase ΔR	n
50 µM	Ca^{2+}, Mg^{2+}-free TRS medium + 1 mM EGTA	0.96 ± 0.22	14
100 µM	Ca^{2+}, Mg^{2+}-free TRS medium + 1 mM EGTA	1.35 ± 0.20[a]	28
200 µM	Ca^{2+}, Mg^{2+}-free TRS medium + 1 mM EGTA	0.88 ± 0,17	14
100 µM	Ca^{2+}, Mg^{2+}-containing TYH medium	1.48 ± 0.24	23
200 µM	Ca^{2+}, Mg^{2+}-containing TYH medium	1.15 ± 0.24	33

[a] Mean value significantly different from ΔR for 50 µM or 200 µM BHQ in Ca^{2+}, Mg^{2+}-free TRS medium + 1 mM EGTA ($p < 0.0001$).

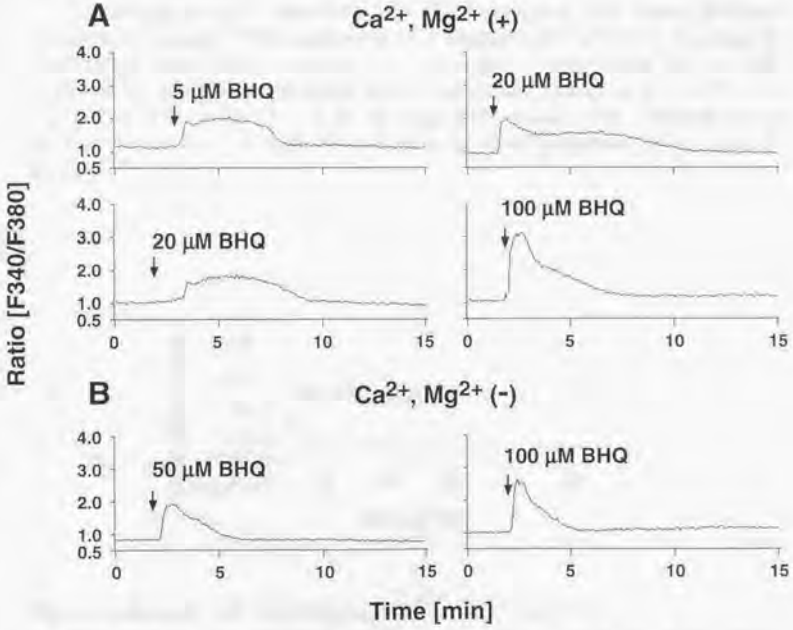

Fig. 4. BHQ induced $[Ca^{2+}]_i$ increase in mouse eggs.

Representative measurement of eggs treated with indicated concentration of BHQ. **A**, eggs were treated with various concentrations of BHQ in normal Ca^{2+}, Mg^{2+}-containing TYH medium (5 µM; n = 7, 20 µM; n = 14, 100 µM; n = 23). **B**, eggs were treated with 50 µM (n = 14) and 100 µM (n = 28) BHQ in Ca^{2+}, Mg^{2+}-free TRS medium containing 1 mM EGTA.

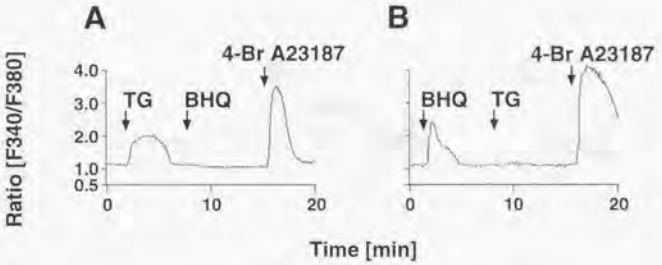

Fig. 5. Thapsigargin and BHQ release Ca^{2+} from the same intracellular store.

Thapsigargin (TG)-sensitive and BHQ-sensitive Ca^{2+} stores overlap extensively in eggs. Two inhibitors were sequentially added to the eggs in Ca^{2+}, Mg^{2+}-free TRS medium. **A**, treatment of eggs with 20 µM TG followed by addition of 100 µM BHQ and treated finally with 5 µM Ca^{2+} ionophore 4-Br A23187 (n = 8). **B**, eggs were treated with 100 µM BHQ prior to addition of 20 µM TG followed by final treatment with 5 µM 4-Br A23187 (n = 11).

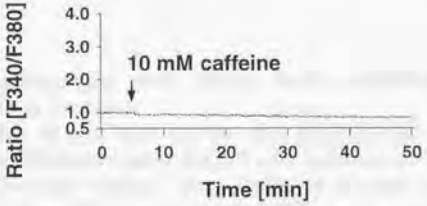

Fig. 6. Absence of caffeine-sensitive Ca^{2+} stores.

There was no marked increase in $[Ca^{2+}]_i$ when eggs were extracellulary treated with caffeine. Eggs were treated with 10 mM caffeine in TYH medium. **A**, representative trace from an unfertilized egg treated with 10 mM caffeine alone (n = 8).

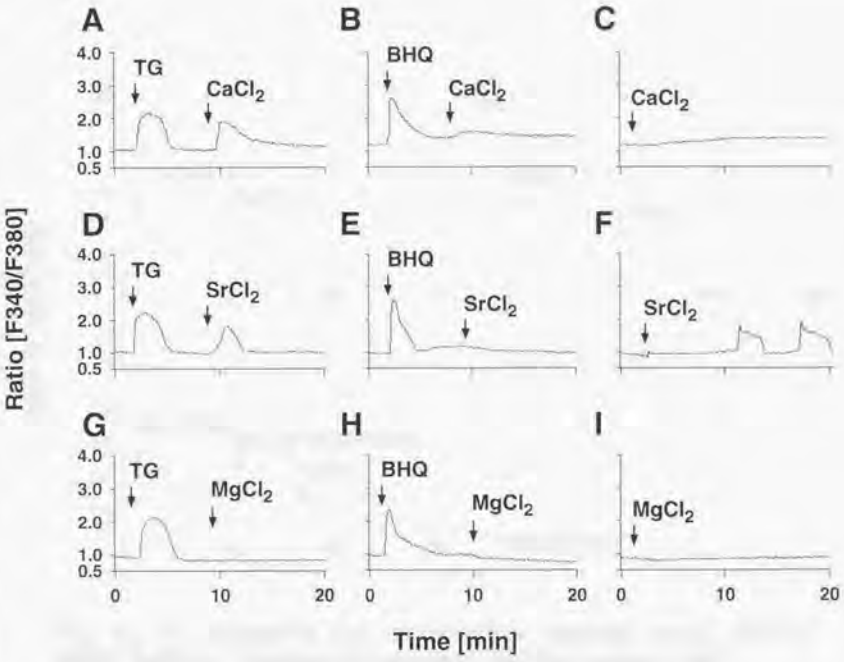

Fig. 7. Thapsigargin and BHQ have different activities on divalent cation entry.

Depletion of the Ca^{2+} stores by thapsigargin (TG) promotes "Capacitative Calcium Entry (CCE)". In contrast to TG, 100 µM BHQ does not induce Ca^{2+} influx. Three different divalent cations were added to Ca^{2+}, Mg^{2+}-free TRS medium containing eggs pretreated with 20 µM TG or 100 µM BHQ. **A**, representative measurement in an egg treated with TG followed by addition of 4.6 mM $CaCl_2$ (n = 5). **B**, an egg treated with BHQ followed by addition of 4.6 mM $CaCl_2$ (n = 9). **C**, control measurement during addition of 4.6 mM $CaCl_2$ alone (n = 14). **D**, treated with TG followed by addition of 4.6 mM $SrCl_2$ (n = 7). **E**, treated with BHQ followed by addition of 4.6 mM $SrCl_2$ (n = 12). **F**, typical measurement following addition of 4.6 mM $SrCl_2$ alone (n = 4). **G**, 4.6 mM $MgCl_2$ were added to the eggs treated with TG (n = 6). **H**, 4.6 mM $MgCl_2$ were added to the eggs treated with BHQ (n = 6). **I**, control experiment of eggs treated with 4.6 mM $MgCl_2$ alone (n = 14).

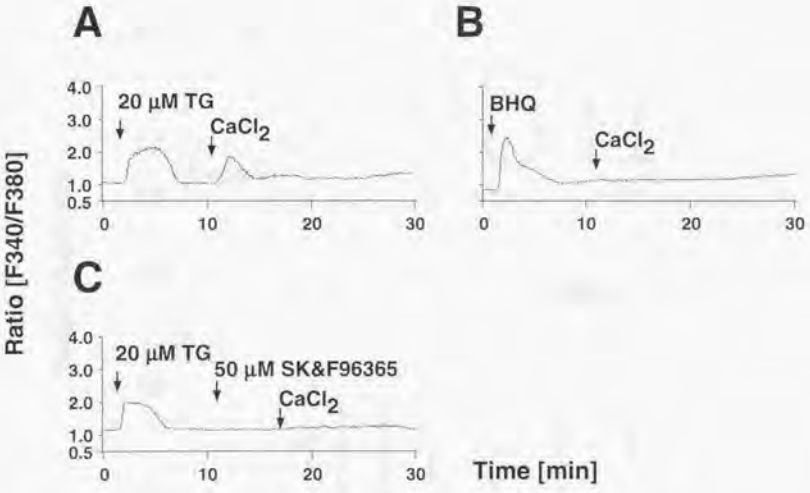

Fig. 8. An antagoist for capacitative calcium entry SK&F 96365 inhibits thapsigargin-induced divalent cation entry.

Capacitative Ca^{2+} entry evoked by thapsigargin (TG) was inhibited by SK&F 96365. **A**, typical measurement in an unfertilized egg treated with 20 μM TG followed by addition of 4.6 mM $CaCl_2$ in Ca^{2+}, Mg^{2+}-free TRS medium containing 1 mM EGTA (n = 9). **B**, representative of an egg treated with 100 μM BHQ followed by addition of 4.6 mM $CaCl_2$ in Ca^{2+}, Mg^{2+}-free TRS medium containing 1 mM EGTA (n = 5). **C**, typical measurement in an unfertilized egg treated with 20 μM TG followed by addition of 50 μM SK&F 96365 and then 4.6 mM $CaCl_2$ in Ca^{2+}, Mg^{2+}-free TRS medium containing 1 mM EGTA (n = 7).

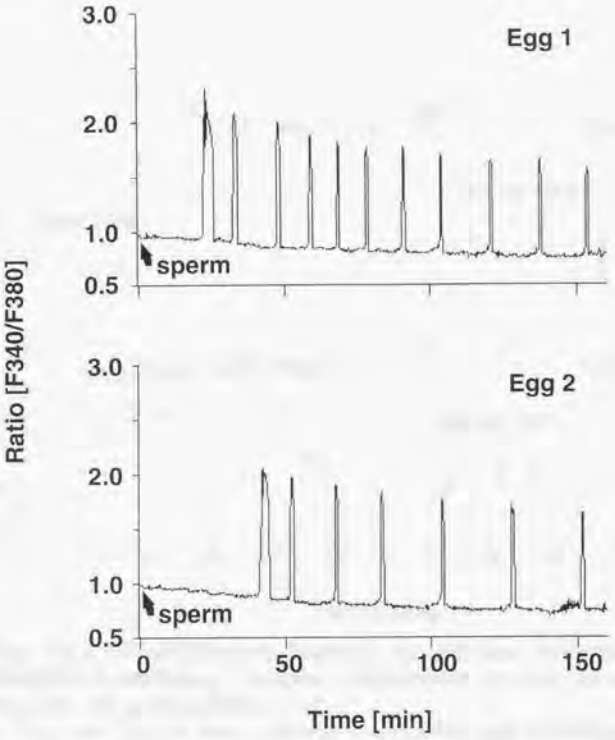

Fig. 9. Ca^{2+} oscillations at fertilization of mouse egg.

Repetitive Ca^{2+} transients occur in mature mouse eggs at fertilization *in vitro*. Eggs from ICR mouse were removed of *Zonae pellucidae* (ZP) and eggs were loaded with fura-2 and inseminated with sperm in TYH medium. Recording of $[Ca^{2+}]_i$ was started (at the zero time) as soon as sperm suspension was added to the drop. Two representative traces made from a same recording and batch of eggs.

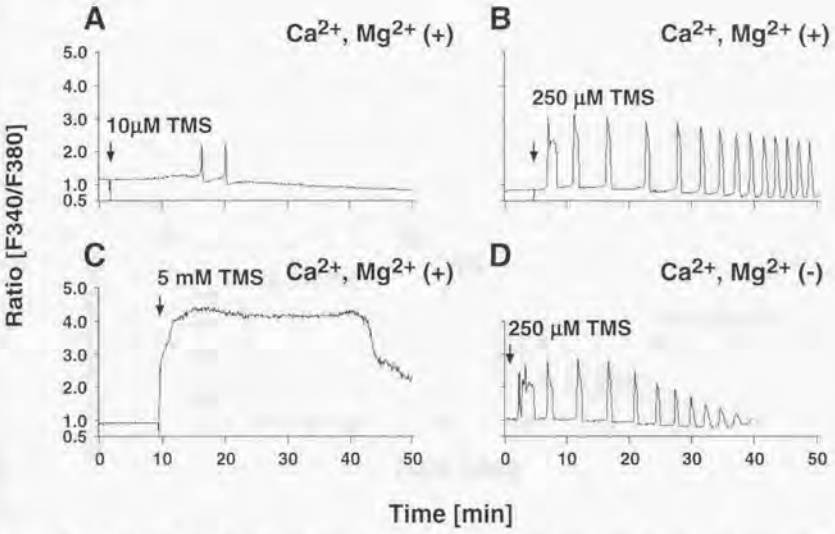

Fig. 10. Ca^{2+} oscillations induced by various concentrations of sulfhydryl-oxidizing reagent thimerosal in the presence and absence of extracellular Ca^{2+}.

Ca^{2+} oscillations were induced by exposing eggs to thimerosal (TMS) both in TYH medium and in Ca^{2+}, Mg^{2+}-free TRS medium. Eggs were treated at the time indicated by the *arrow* with various concentrations of TMS. **A**, 10 μM (n = 6). **B**, 250 μM (n = 12). **C**, 5 mM (n = 12) in TYH medium containing 1.7 mM $CaCl_2$. **D**, 250 μM in Ca^{2+}, Mg^{2+}-free TRS medium (n = 7).

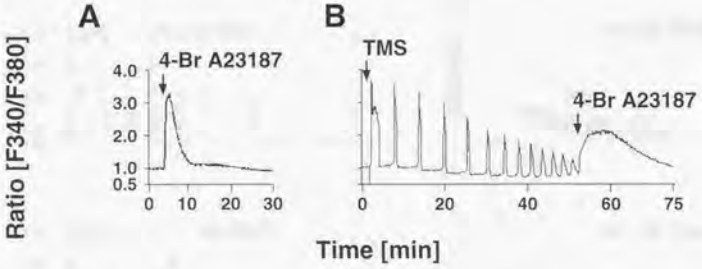

Fig. 11. Thimerosal depletes a large part of intracellular Ca^{2+} stores.

Significant proportion of Ca^{2+} stores are depleted by thimerosal-induced oscillation. **A**, control experiment of eggs treated with 5 µM 4-Br A23187 alone (n = 25). **B**, 5 µM 4-Br A23187 was added after stimulation of eggs with 250 µM TMS in Ca^{2+}, Mg^{2+}-free TRS medium (n = 27).

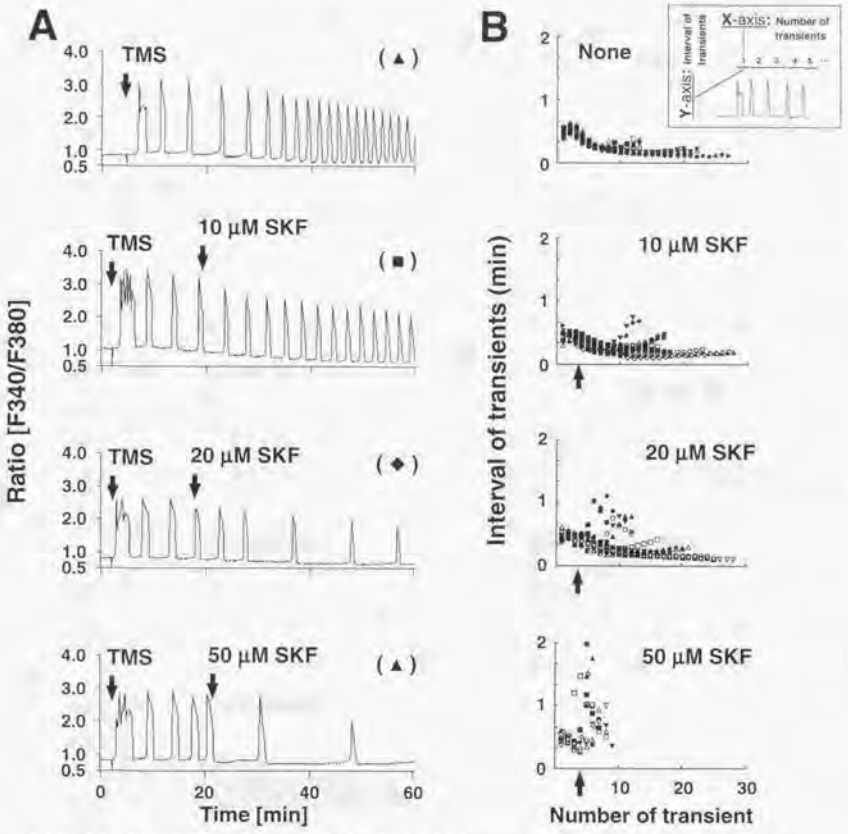

Fig. 12. Ca^{2+} antagonist SK&F 96365 suppresses the frequency of thimerosal-induced Ca^{2+} oscillations.

SK&F 96365 modulates the frequency of thimerosal (TMS)-induced Ca^{2+} oscillations in the presence of external Ca^{2+}. Dose-dependent inhibition of frequency of Ca^{2+} oscillations induced by TMS. **A**, representative traces of eggs (shown with the same *symbol* in B) from a batch shown in B (*right panel*). Eggs were treated with indicated concentration of SK&F 96365 after induction of Ca^{2+} transients with 250 µM TMS in TYH medium (none; n = 12, 10 µM; n = 24, 20 µM; n = 23, 50 µM; n = 51). **B**, interval of the transients (*y axis*) were calculated between the peak of the transients and plotted against number of transients (*x axis*) occured during 1 h of measurement (none; n = 12, 10 µM; n = 13, 20 µM; n = 12, 50 µM; n = 10). SK&F 96365 was added to the medium at the point indicated by the *arrow*. Number of transients are decreased and periods between the transients are prolonged with the increasing dose of the antagonist. One experiment representative of two to four is shown.

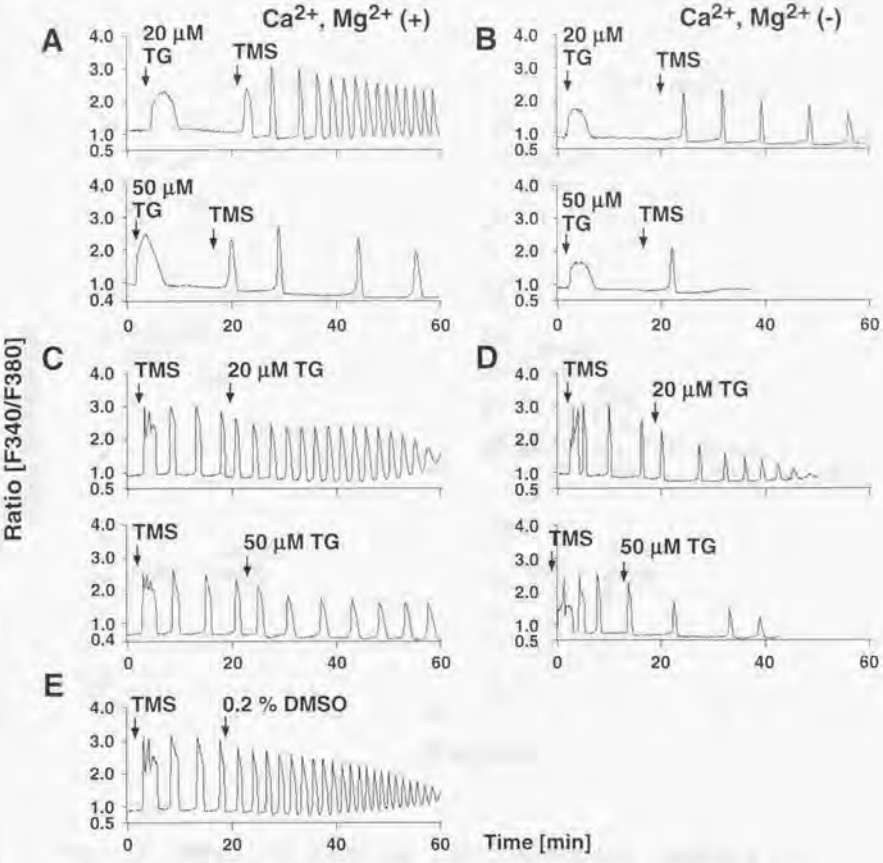

Fig. 13. Effect of thapsigargin on Ca^{2+} oscillations induced by thimerosal.

Thapsigargin (TG) has an inhibitory effect on the oscillation induced by thimerosal (TMS). TG was added before and after the stimulation of Ca^{2+} oscillations induced by 250 µM TMS in the presence and absence of external Ca^{2+}. **A**, eggs were treated with 20 µM (*upper trace*, n = 18) and 50 µM (*lower trace*, n = 25) TG followed by addition of TMS in TYH medium. **B**, treated with 20 µM (*upper trace*, n = 17) and 50 µM (*lower trace*, n = 13) TG in Ca^{2+}, Mg^{2+}-free TRS medium containing 1 mM EGTA prior to stimulation with TMS. **C**, representative measurement of TMS stimulated egg treated with 20 µM (*upper trace*, n = 19) and 50 µM TG (*lower trace*, n = 22). **D**, eggs were treated with TMS followed by addition of 20 µM (*upper trace*, n = 8) in Ca^{2+}, Mg^{2+}-free TRS medium and 50 µM TG (*lower trace*, n = 5) in Ca^{2+}, Mg^{2+}-free TRS medium containing 1 mM EGTA. **E**, control measurement of 250 µM TMS stimulated egg treated with 0.2 % DMSO in TYH medium (n = 7).

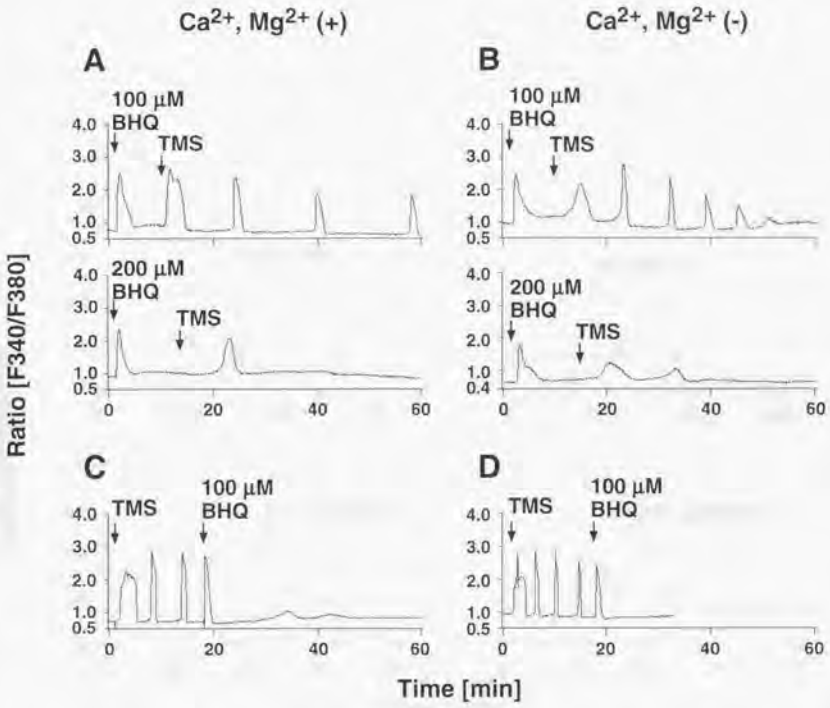

Fig. 14. Effect of BHQ on Ca^{2+} oscillations induced by thimerosal.

BHQ inhibits thimerosal (TMS)-induced Ca^{2+} oscillations when added after stimulation by TMS. BHQ (100 µM) was added before and after the stimulation of Ca^{2+} oscillations induced by 250 µM TMS in the presence and absence of external Ca^{2+}. **A**, eggs were treated with 100 µM (*upper trace*, n = 22) and 200 µM (*lower trace*, n = 17) BHQ followed by addition of TMS in normal Ca^{2+}-containing TYH medium. **B**, typical measurement of eggs treated with 100 µM (*upper trace*, n = 13) and 200 µM (*lower trace*, n = 14) BHQ after stimulation with TMS in Ca^{2+}, Mg^{2+}-free TRS medium containing 1 mM EGTA. **C** and **D**, 100 µM BHQ was added to the eggs previously stimulated with TMS in TYH medium (n = 16) and in Ca^{2+}, Mg^{2+}-free TRS medium (n = 21) respectively.

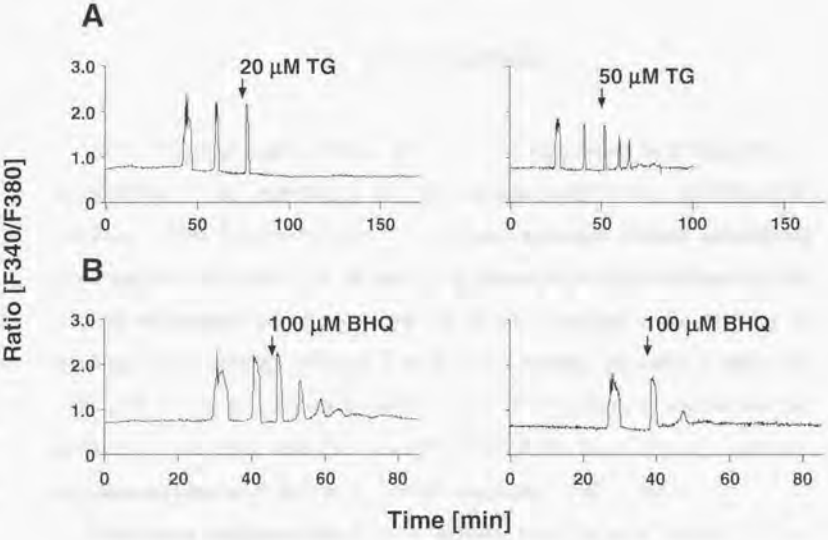

Fig. 15. Effect of Ca^{2+}-ATPase inhibitors on sperm induced Ca^{2+} oscillations.

Thapsigargin (TG) and BHQ both suppressed Ca^{2+} transients following fertilization. **A**, two different representative traces of eggs inseminated and treated with 20 µM (n = 6) and 50 µM (n = 4) TG after the second transient increase in $[Ca^{2+}]_i$ induced by sperm (*left trace*; 3/10, *right trace*; 1/10). **B** (n = 7), two different representative $[Ca^{2+}]_i$ measurements (*left trace*; 2/7, *right trace*; 5/7) in which fertilized eggs were treated with 100 µM BHQ in TYH medium after fertilization.

Chapter III

Cortical granule exocytosis in mouse egg

1. Introduction

In mammalian eggs, cortical granule (CG) exocytosis at fertilization is considered to be important for preventing polyspermic fertilization (Gulyas, 1979). Exocytosis of CGs, secretory granules contain specialized enzymes and glycoproteins, is caused by fusion of their membranes to the plasma membrane, resulting in release of CG contents at the surface of the eggs. The contents released from the CGs modify the *zonae pellucidae* (ZP) and result in a block to polyspermy. The exduates remain on the surface of the eggs and they can be labeled by LCA (*Lens culinaris aggulutinin)*-lectin (Cherr *et al.*, 1988; Ducibella *et al.*, 1988).

It has been suggested that $[Ca^{2+}]_i$ increase is essential for early and late events in mouse eggs at fertilization (Kline and Kline, 1992a; Xu *et al.*, 1996). Higher concentrations of calcium chelator; BAPTA-AM is required to inhibit CG exocytosis than to inhibit emmision of the second PB (Kline and Kline, 1992a). By injecting Ca^{2+}-BAPTA buffers into unfertilized eggs, it was suggested that CG exocytosis occurs over a narrow threshold range of free-Ca^{2+} concentrations (Xu *et al.*, 1996). Results of these studies suggest that early events of egg activation such as CG exocytosis are more sensitive to experimental manipulation than the late events. I have previously demonstrated that treatment of eggs with thapsigargin (TG) and BHQ resulted in transient increase in $[Ca^{2+}]_i$ from the intracellular stores (Figure 3, 4 and Table 1). In this chapter, I

examined whether these increase in $[Ca^{2+}]_i$ by Ca^{2+}-ATPase inhibitors can induce CG exocytosis in eggs.

2. Materials and methods

Drug treatment

ZP-free mature eggs were treated with various concentration of the inhibitors for 30 min at 37 ˚C in a 200 μl drop of TYH medium. Eggs were washed extensively with TYH medium and held in the drop of TYH medium, under mineral oil.

Labeling the cortical granule exudate with LCA (Lens culinaris agglutinin) and visualization of egg chromatin

Unfixed eggs were washed in TYH medium and incubated for 15 min at 37 ˚C in 10 μg/ml fluorescein isothiocyanate (FITC)-conjugated LCA (Seikagaku Corp., Tokyo, Japan) in TYH medium. These eggs were thoroughly washed and viewed with a standard epifluorescence microscopy (Axiophot 2; Carl Zeiss, Jena, Germany). To visualize the egg chromatin, a DNA-specific fluorochrome, Hoechst 33342 (Sigma) was used. Preloading the eggs with Hoechst dyes before insemination allowed detection of sperm-egg fusion (Conover and Gwatkin, 1988). Unfertilized eggs were incubated in 0.5 μg/ml Hoechst 33342 in TYH medium at 37 ˚C for 15 min and washed with TYH medium before insemination.

3. Results

3.1 Cortical granule exocytosis at fertilization and activation of mouse eggs

3.1.1 Sperm and Ca^{2+} ionophore-induced cortical granule exocytosis in eggs

CG exocytosis at fertilization and artificial activation by 4-Br A23187 were evaluated by LCA staining indicated under Materials and Methods. Two hour after fertilization, as shown in Figure 16A, most eggs extruded second polar body (PB) and were penetrated by one or more sperm indicated by Hoechst staining (Figure 16C). These eggs underwent exocytosis as indicated by CG exduate identified with FITC-LCA (Figure 16B). CG exocytosis can be induced by artificial activators, such as Ca^{2+} ionophore and $SrCl_2$. As shown in Figure 16E, exocytosis occured in all eggs treated with Ca^{2+} ionophore 4-Br A23187 (5 μM) in Ca^{2+}, Mg^{2+}-free TRS medium.

3.2 Cortical granule exocytosis induced by Ca^{2+}-ATPase inhibitors

3.1.2 Effect of thapsigargin and BHQ on cortical granule exocytosis in eggs

Eggs treated with TG concentration of 20 μM which induces maximal Ca^{2+} release from the stores resulted in CG exocytosis in 79 % (26/33) of the treated eggs (n = 33). Representative eggs treated with 20 μM TG are shown in Figure 17C and D. Treatment of eggs with BHQ concentration

of 100 μM caused CG exocytosis in 88 % (15/17) of the eggs (Figure 17F, n = 8). These eggs treated with inhibitors showed positive staining with FITC-LCA as compared to eggs treated with 0.2 % DMSO (Figure 17B, n = 10), however, the intensity of the FITC-LCA fluorescence was weak as compared to the eggs activated by Ca^{2+} ionophore and sperm. Treatment of eggs with 5 μM (n = 7) and 20 μM (n = 14) BHQ, concentrations that did not cause maximal Ca^{2+} release (Figure 4A) showed no staining at all (data not shown). Moreover, raising the concentrations of BHQ to 200 μM, only 50 % (4/8) of the eggs resulted in exocytosis (n = 8; data not shown). The parallelism between the BHQ concentration and the proportion of the eggs resulted in CG exocytosis suggest that triggering of CG exocyotsis is dependent on the Ca^{2+} concentration in the cytosol.

Metaphase II-arrested eggs possess a CG-free domain that contains the chromosomes and an opposing CG-rich domain containing a high density of CGs. As shown in Figure 18, fertilized egg showed the ring-shaped pattern of immunofluorescence stained with FITC-LCA. I next observed the eggs which were treated with 20 μM TG or 100 μM BHQ using laser-scanning confocal microscope to see the precise pattern of staining. As shown in Figure 19 (n = 2), FITC-LCA fluorescence was observed around the plasma membrane of the eggs and formed a ring-shaped band similar to the eggs underwent CG exocytosis induced by fertilization. Same experiment was done with the eggs treated with 100 μM BHQ (Figure 20, n = 3). These eggs also showed typical staining pattern seen with fertilized eggs. Spatial pattern of CG exocytosis induced by Ca^{2+}-ATPase inhibitors was not different from those induced by fertilization.

4. Discussion

4.1 Cortical granule exocytosis and Ca^{2+} concentrations in eggs.

Eggs treated with TG and BHQ exhibited exocytosis of CGs, as assessed with FITC-LCA staining method. Moreover, thapsigargin and BHQ treated eggs showed typical staining pattern of CGs (Figure 19 and 20). Thimerosal treated eggs showed exocytosis (data not shown) consistent with the previous result (Cheek *et al.*, 1993). However, the low fluorescence intensity was observed with eggs treated with those inhibitors (Figure 17) compared to the eggs fertilized or activated with Ca^{2+} ionophore (Figure 16). Moreover, as demonstrated in Figure 3 and 4, although I have induced maximal Ca^{2+} release with these inhibitors, BHQ treated eggs showed much low fluorescence intensity than thapsigargin treated eggs (Figure 17F). It is possible that completion of CG exocytosis in eggs requires not only the transient increase in $[Ca^{2+}]_i$ above the threshold, but the repeated increase in $[Ca^{2+}]_i$, like induced by sperm (Figure 9) and thimerosal (Figure 10B) or sustained level of increase for few minutes, like induced by Ca^{2+} ionophore (Figure 11A), since elevation of $[Ca^{2+}]_i$ by thapsigargin lasted longer than that of BHQ (Figure 3 and 4) but relatively shorter than that of Ca^{2+} ionophore (Figure 11). The Ca^{2+}-ATPase inhibitors will be very useful to control the Ca^{2+} concentration in the cyotsol and examine the threshold of Ca^{2+} concentration that triggers the CG exocytosis. Studying the parallelism between the Ca^{2+} concentration and the proportion of the eggs underwent CG exocytosis may provide the evidence for the dependence of CG exocytosis on Ca^{2+} concentration in the cytosol.

Although, it is quite clear that Ca^{2+} plays a key role in CG exocytosis, molecular target of Ca^{2+} is not defined. It has been shown that the CG exocytosis in mouse egg occures constitutively and continued at almost uniform rate for tens of minutes after the sperm attachment, and was not always induced concomitantly with each $[Ca^{2+}]_i$ increase (Tahara *et al.*, 1996). Increase of intracellular Ca^{2+} concentration can be the trigger of the exocytosis, however, such results from experiment by Tahara et. al. indicates the presence of messenger other than Ca^{2+}. The next step of the Ca^{2+}-dependent pathway in CG exocytosis remains unknown. It has been suggested that W-7, an antagonist of calmodulin, did not affect exocytosis (Xu *et al.*, 1996). I have also observed the same effect using the same inhibitor and another specific inhibitor for calmodulin (unpublished results). These results indicate that the mechanisms of CG exocytosis may not depend on the Ca^{2+}/calmodulin-dependent pathway.

5. Figures

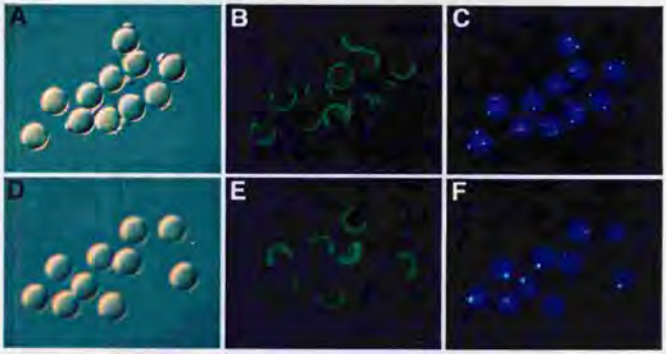

Fig. 16. Cortical granule exocytosis at fertilization and activation of mouse egg.

Cortical granule (CG) exocytosis occur in mature mouse eggs at fertilization *in vitro* and activation by Ca^{2+} ionophore. ZP-free mouse eggs were incubated with FITC-LCA in TYH medium 40 min after insemination or activation with Ca^{2+} ionophore and observed at 2 h post treatment. **A**, differential interference contrast (DIC) image of eggs after fertilization (n = 11). **B**, FITC-LCA fluorescent image of eggs in same field as in A. **C**, eggs in same field as in A and B were stained with Hoechst 33342 (0.5 µg/ml). **D**, DIC image of eggs which were artificially activated with 5 µM 4-Br A23187 (n = 10). **E**, FITC-LCA fluorescent image of eggs in same field as

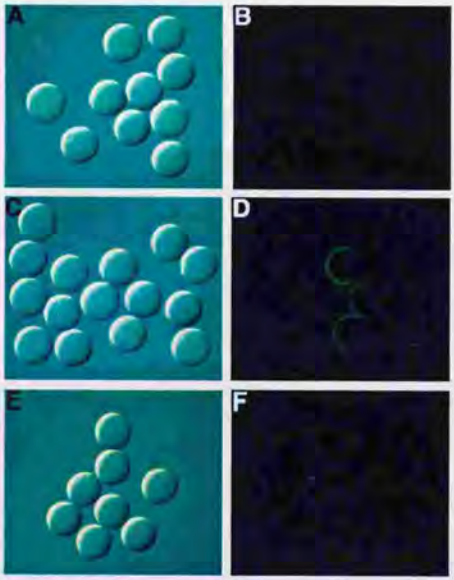

Fig. 17. Cortical granule exocytosis induced by Ca^{2+}-ATPase inhibitors in mouse egg.

CG exocytosis occur in mature mouse eggs treated with thapsigargin (TG) and BHQ. Eggs treated with the inhibitors were incubated with FITC-LCA and observed at 2 h post treatment. **A**, differential interference contrast (DIC) image of eggs pretreated with 0.2 % DMSO (n = 10). **B**, FITC-LCA fluorescent image of eggs in same field as in A. **C**, DIC image of eggs pretreated with 20 µM TG (n = 15). **D**, FITC-LCA fluorescent image of same field as in C. **E**, DIC image of eggs pretreated with 100 µM BHQ (n = 8). **F**, FITC-LCA fluorescent image of same field as in E.

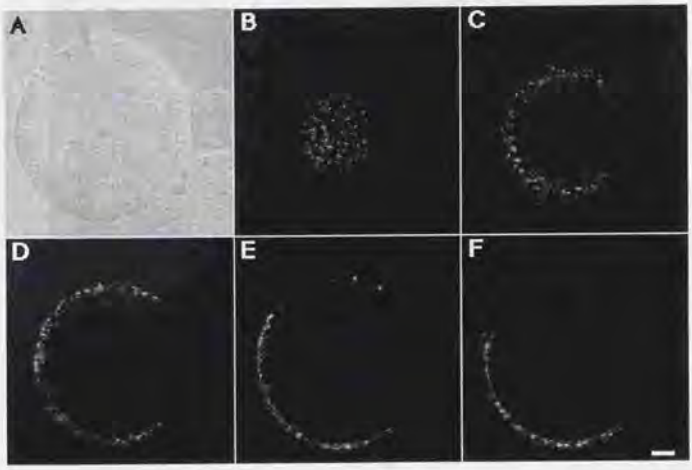

Fig. 18. Confocal sections of fertilized egg stained for exocytosed cortical granule exduates.

Eggs were fertilized and incubated with FITC-LCA and viewed with laser-scanning confocal microscope at 2 h after insemination. **A**, DIC image of fertilized egg which have extruded the second polar body. **B**, optical sections (approximately 5 μm depth) viewed at the bottom of the egg. **C**, an optical section at approximately 10 μm from the bottom. **D**, 20 μm from the bottom. **E**, 30 μm from the bottom. **F**, 40 μm from the bottom. Scale bar represents 10 μm.

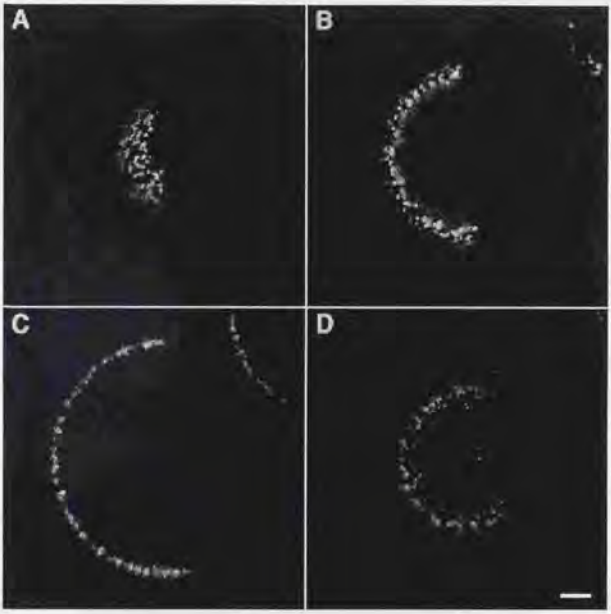

Fig. 19. Confocal sections of thapsigargin treated eggs stained with FITC-LCA.

Thapsigargin (TG)-treated eggs showed a typical discharge of the CG content. Eggs were treated with 20 µM TG for 30 min in TYH medium and incubated with FITC-LCA and viewed with laser-scanning confocal microscope at 2 h after the treatment (n = 2). **A**, an optical section (approximately 5 µm depth) viewed at the bottom of the egg. **B**, an optical section at approximately 10 µm from the bottom. **C**, 30 µm from the bottom. **D**, an optical section approximately 70 µm from the bottom. Scale bar represents 10 µm.

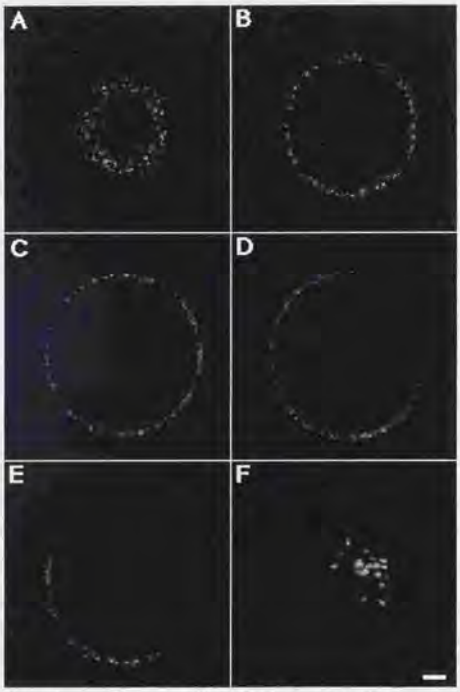

Fig. 20. Confocal sections of BHQ treated eggs stained with FITC-LCA.

Eggs treated with BHQ also showed a typical discharge of the CG exduate. Eggs were treated with 100 μM BHQ for 30 min in TYH medium. Hoechst 33342 was loaded and incubated with FITC-LCA and viewed with laser-scanning confocal microscope at 2 h after the treatment (n = 3). **A**, an optical section (approximately 5 μm depth) viewed at the bottom of the egg. **B**, an optical section at approximately 10 μm from the bottom. **C**, 20 μm from the bottom. **D**, an optical section approximately 30 μm from the bottom. **E**, 40 μm from the bottom. **F**, a fluorescent image of chromosome stained with Hoechst 33342. Scale bar represents 10 μm.

References

Bement, W. M. (1992). Signal transduction by calcium and protein kinase C during egg activation. [Review] [114 refs]. *Journal of Experimental Zoology* **263,** 382-97.

Berridge, M. J., and Galione, A. (1988). Cytosolic calcium oscillators. [Review] [49 refs]. *Faseb Journal* **2,** 3074-82.

Bian, J. H., Ghosh, T. K., Wang, J. C., and Gill, D. L. (1991). Identification of intracellular calcium pools. Selective modification by thapsigargin. *Journal of Biological Chemistry* **266,** 8801-6.

Blondel, O., Takeda, J., Janssen, H., Seino, S., and Bell, G. I. (1993). Sequence and functional characterization of a third inositol trisphosphate receptor subtype, IP_3R-3, expressed in pancreatic islets, kidney, gastrointestinal tract, and other tissues. *Journal of Biological Chemistry* **268,** 11356-11363.

Bootman, M. D., Taylor, C. W., and Berridge, M. J. (1992). The thiol reagent, thimerosal, evokes Ca^{2+} spikes in HeLa cells by sensitizing the inositol 1,4,5-trisphosphate receptor. *Journal of Biological Chemistry* **267,** 25113-9.

Cascio, S. M., and Wassarman, P. M. (1982). Program of early development in the mammal: post-transcriptional control of a class of proteins synthesized by mouse oocytes and early embryos. *Developmental Biology* **89,** 397-408.

Cheek, T. R., McGuinness, O. M., Vincent, C., Moreton, R. B., Berridge, M. J., and Johnson, M. H. (1993). Fertilisation and thimerosal stimulate similar calcium spiking patterns in mouse oocytes but by separate mechanisms. *Development* **119,** 179-89.

Cherr, G. N., Drobnis, E. Z., and Katz, D. F. (1988). Localization of cortical granule constituents before and after exocytosis in the hamster egg. *Journal of Experimental Zoology* **246,** 81-93.

Chini, E. N., Beers, K. W., and Dousa, T. P. (1995). Nicotinate adenine dinucleotide phosphate (NAADP) triggers a specific calcium release system in sea urchin eggs [published erratum appears in J Biol Chem 1995 Apr 28;270(17):10359]. *Journal of Biological Chemistry* **270,** 3216-23.

Ciapa, B., and Epel, D. (1991). A rapid change in phosphorylation on tyrosine accompanies fertilization of sea urchin eggs. *FEBS Letters* **295,** 167-70.

Conover, J. C., and Gwatkin, R. B. (1988). Pre-loading of mouse oocytes with DNA-specific fluorochrome (Hoechst 33342) permits rapid detection of sperm-oocyte fusion. *Journal of Reproduction and Fertility* **82,** 681-90.

Cuthbertson, K. S. (1983). Parthenogenetic activation of mouse oocytes in vitro with ethanol and benzyl alcohol. *Journal of Experimental Zoology* **226,** 311-4.

Demaurex, N., Lew, D. P., and Krause, K. H. (1992). Cyclopiazonic acid depletes intracellular Ca^{2+} stores and activates an influx pathway for divalent cations in HL-60 cells. *Journal of Biological Chemistry* **267,** 2318-24.

Ducibella, T., Anderson, E., Albertini, D. F., Aalberg, J., and Rangarajan, S. (1988). Quantitative studies of changes in cortical granule number and distribution in the mouse oocyte during meiotic maturation. *Developmental Biology* **130,** 184-97.

Dupont, G., McGuinness, O. M., Johnson, M. H., Berridge, M. J., and Borgese, F. (1996). Phospholipase C in mouse oocytes: characterization of beta and gamma isoforms and their possible involvement in sperm-induced Ca^{2+} spiking. *Biochemical Journal* **316,** 583-91.

Ely, J. A., Ambroz, C., Baukal, A. J., Christensen, S. B., Balla, T., and Catt, K. J. (1991). Relationship between agonist- and thapsigargin-sensitive calcium pools in adrenal glomerulosa cells. Thapsigargin-induced Ca^{2+} mobilization and entry. *Journal of Biological Chemistry* **266,** 18635-41.

Endo, Y., Kopf, G. S., and Schultz, R. M. (1986). Stage-specific changes in protein phosphorylation accompanying meiotic maturation of mouse oocytes and fertilization of mouse eggs. *Journal of Experimental Zoology* **239,** 401-9.

Ferris, C. D., Huganir, R. L., Supattapone, S., and Snyder, S. H. (1989). Purified inositol 1,4,5-trisphosphate receptor mediates calcium flux in reconstituted lipid vesicles. *Nature* **342,** 87-9.

Fissore, R. A., Dobrinsky, J. R., Balise, J. J., Duby, R. T., and Robl, J. M. (1992). Patterns of intracellular Ca^{2+} concentrations in fertilized bovine eggs. *Biology of Reproduction* **47,** 960-9.

Foskett, J. K., Roifman, C. M., and Wong, D. (1991). Activation of calcium oscillations by thapsigargin in parotid acinar cells. *Journal of Biological Chemistry* **266,** 2778-82.

Foskett, J. K., and Wong, D. (1992). Calcium oscillations in parotid acinar cells induced by microsomal Ca^{2+}-ATPase inhibition. *American Journal of Physiology* **262,** C656-63.

Furuichi, T., Yoshikawa, S., Miyawaki, A., Wada, K., Maeda, N., and Mikoshiba, K. (1989). Primary structure and functional expression of the inositol 1,4,5-trisphosphate-binding protein P400. *Nature* **342,** 32-8.

Genazzani, A. A., and Galione, A. (1996). Nicotinic acid-adenine dinucleotide phosphate mobilizes Ca^{2+} from a thapsigargin-insensitive pool. *Biochemical Journal* **315,** 721-5.

Gulyas, B. J. (1979). Cortical granules of mammalian eggs. [Review] [134 refs]. *International Review of Cytology* **63,** 357-92.

Hatzelmann, A., Haurand, M., and Ullrich, V. (1990). Involvement of calcium in the thimerosal-stimulated formation of leukotriene by fMLP in human polymorphonuclear leukocytes. *Biochemical Pharmacology* **39,** 559-67.

Hecker, M., Brune, B., Decker, K., and Ullrich, V. (1989). The sulfhydryl reagent thimerosal elicits human platelet aggregation by mobilization of intracellular calcium and secondary prostaglandin endoperoxide formation. *Biochemical & Biophysical Research Communications* **159,** 961-8.

Howlett, S. K. (1986). A set of proteins showing cell cycle dependent modification in the early mouse embryo. *Cell* **45,** 387-96.

Igusa, Y., and Miyazaki, S. (1983). Effects of altered extracellular and intracellular calcium concentration on hyperpolarizing responses of the hamster egg. *Journal of Physiology* **340,** 611-32.

Jackson, T. R., Patterson, S. I., Thastrup, O., and Hanley, M. R. (1988). A novel tumour promoter, thapsigargin, transiently increases cytoplasmic free Ca^{2+} without generation of inositol phosphates in NG115-401L neuronal cells. *Biochemical Journal* **253,** 81-6.

Jaffe, L. A., Sharp, A. P., and Wolf, D. P. (1983). Absence of an electrical polyspermy block in the mouse. *Developmental Biology* **96,** 317-23.

Jones, K. T., Carroll, J., Merriman, J. A., Whittingham, D. G., and Kono, T. (1995). Repetitive sperm-induced Ca^{2+} transients in mouse oocytes are cell cycle dependent. *Development* **121,** 3259-66.

Kass, G. E., Duddy, S. K., Moore, G. A., and Orrenius, S. (1989). 2,5-Di-(tert-butyl)-1,4-benzohydroquinone rapidly elevates cytosolic Ca^{2+} concentration by mobilizing the inositol 1,4,5-trisphosphate-sensitive Ca^{2+} pool. *Journal of Biological Chemistry* **264,** 15192-8.

Kline, D., and Kline, J. T. (1992a). Repetitive calcium transients and the role of calcium in exocytosis and cell cycle activation in the mouse egg. *Developmental Biology* **149,** 80-9.

Kline, D., and Kline, J. T. (1992b). Thapsigargin activates a calcium influx pathway in the unfertilized mouse egg and suppresses repetitive calcium transients in the fertilized egg. *Journal of Biological Chemistry* **267,** 17624-30.

Kline, J. T., and Kline, D. (1994). Regulation of intracellular calcium in the mouse egg: evidence for inositol trisphosphate-induced calcium release, but not calcium-induced calcium release. *Biology of Reproduction* **50,** 193-203.

Kume, S., Muto, A., Aruga, J., Nakagawa, T., Michikawa, T., Furuichi, T., Nakade, S., Okano, H., and Mikoshiba, K. (1993). The Xenopus IP_3 Receptor: Structure, Function, and Localization in Oocytes and Eggs. *Cell* **73,** 555-570.

Laemmli, U. K. (1970). Cleavage of structural proteins during the assembly of the head of bacteriophage T4. *Nature* **227,** 680-5.

Law, G. J., Pachter, J. A., Thastrup, O., Hanley, M. R., and Dannies, P. S. (1990). Thapsigargin, but not caffeine, blocks the ability of thyrotropin-releasing hormone to release Ca^{2+} from an intracellular store in GH4C1 pituitary cells. *Biochemical Journal* **267,** 359-64.

Llopis, J., Chow, S. B., Kass, G. E., Gahm, A., and Orrenius, S. (1991). Comparison between the effects of the microsomal Ca^{2+}-translocase inhibitors thapsigargin and 2,5-di-(t-butyl)-1,4-benzohydroquinone on cellular calcium fluxes. *Biochemical Journal* **277,** 553-6.

Lytton, J., Westlin, M., and Hanley, M. R. (1991). Thapsigargin inhibits the sarcoplasmic or endoplasmic reticulum Ca^{2+}-ATPase family of calcium pumps. *Journal of Biological Chemistry* **266,** 17067-71.

Maeda, N., Kawasaki, T., Nakade, S., Yokota, N., Taguchi, T., Kasai, M., and Mikoshiba, K. (1991). Structural and functional characterization of

inositol 1,4,5-trisphosphate receptor channel from mouse cerebellum. *Journal of Biological Chemistry* **266,** 1109-16.

Maranto, A. R. (1994). Primary structure, ligand binding, and localization of the human type 3 inositol 1,4,5-trisphosphate receptor expressed in intestinal epithelium. *Journal of Biological Chemistry* **269,** 1222-30.

Mason, M. J., Garcia-Rodriguez, C., and Grinstein, S. (1991). Coupling between intracellular Ca^{2+} stores and the Ca^{2+} permeability of the plasma membrane. Comparison of the effects of thapsigargin, 2,5-di-(*tert*-butyl)-1,4-hydroquinone, and cyclopiazonic acid in rat thymic lymphocytes. *Journal of Biological Chemistry* **266,** 20856-62.

Mehlmann, L. M., Mikoshiba, K., and Kline, D. (1996). Redistribution and increase in cortical inositol 1,4,5-trisphosphate receptors after meiotic maturation of the mouse oocyte. *Developmental Biology* **180,** 489-98.

Mehlmann, L. M., Terasaki, M., Jaffe, L. A., and Kline, D. (1995). Reorganization of the endoplasmic reticulum during meiotic maturation of the mouse oocyte. *Developmental Biology* **170,** 607-15.

Merritt, J. E., Armstrong, W. P., Benham, C. D., Hallam, T. J., Jacob, R., Jaxa-Chamiec, A., Leigh, B. K., McCarthy, S. A., Moores, K. E., and Rink, T. J. (1990). SK&F 96365, a novel inhibitor of receptor-mediated calcium entry. *Biochemical Journal* **271,** 515-22.

Mignery, G. A., Newton, C. L., Archer, B. 3., and Sudhof, T. C. (1990). Structure and expression of the rat inositol 1,4,5-trisphosphate receptor. *Journal of Biological Chemistry* **265,** 12679-85.

Missiaen, L., De Smedt, H., Droogmans, G., and Casteels, R. (1992). Ca^{2+} release induced by inositol 1,4,5-trisphosphate is a steady-state phenomenon controlled by luminal Ca^{2+} in permeabilized cells. *Nature* **357,** 599-602.

Missiaen, L., Wuytack, F., Raeymaekers, L., De Smedt, H., Droogmans, G., Declerck, I., and Casteels, R. (1991). Ca^{2+} extrusion across plasma membrane and Ca^{2+} uptake by intracellular stores. [Review] [493 refs]. *Pharmacological Therapeutics* **50,** 191-232.

Miyawaki, A., Furuichi, T., Maeda, N., and Mikoshiba, K. (1990). Expressed cerebellar-type inositol 1,4,5-trisphosphate receptor, P400, has calcium release activity in a fibroblast L cell line. *Neuron* **5,** 11-8.

Miyazaki, S. (1988). Inositol 1,4,5-trisphosphate-induced calcium release and guanine nucleotide-binding protein-mediated periodic calcium rises in golden hamster eggs. *Journal of Cell Biology* **106,** 345-53.

Miyazaki, S. (1991). Repetitive calcium transients in hamster oocytes. [Review] [43 refs]. *Cell Calcium* **12,** 205-16.

Miyazaki, S., Shirakawa, H., Nakada, K., Honda, Y., Yuzaki, M., Nakade, S., and Mikoshiba, K. (1992a). Antibody to the inositol trisphosphate receptor blocks thimerosal-enhanced Ca^{2+}-induced Ca^{2+} release and Ca^{2+} oscillations in hamster eggs. *FEBS Letters* **309,** 180-4.

Miyazaki, S., Yuzaki, M., Nakada, K., Shirakawa, H., Nakanishi, S., Nakade, S., and Mikoshiba, K. (1992b). Block of Ca^{2+} wave and Ca^{2+} oscillation by antibody to the inositol 1,4,5-trisphosphate receptor in fertilized hamster eggs [published erratum appears in Science 1992 Oct 9;258(5080):following 203]. *Science* **257,** 251-5.

Monkawa, T., Miyawaki, A., Sugiyama, T., Yoneshima, H., Yamamoto-Hino, M., Furuichi, T., Saruta, T., Hasegawa, M., and Mikoshiba, K. (1995). Heterotetrameric complex formation of inositol 1,4,5-trisphosphate receptor subunits. *Journal of Biological Chemistry* **270,** 14700-14704.

Moore, G. A., McConkey, D. J., Kass, G. E., O'Brien, P. J., and Orrenius, S. (1987). 2,5-Di(*tert*-butyl)-1,4-benzohydroquinone--a novel inhibitor of liver microsomal Ca^{2+} sequestration. *FEBS Letters* **224,** 331-6.

Parrington, J., Swann, K., Shevchenko, V. I., Sesay, A. K., and Lai, F. A. (1996). Calcium oscillations in mammalian eggs triggered by a soluble sperm protein. *Nature* **379,** 364-8.

Petersen, C. C., and Berridge, M. J. (1994). The regulation of capacitative calcium entry by calcium and protein kinase C in Xenopus oocytes. *Journal of Biological Chemistry* **269,** 32246-53.

Putney, J., Jr. (1986). A model for receptor-regulated calcium entry. [Review] [37 refs]. *Cell Calcium* **7,** 1-12.

Putney, J., Jr. (1990). Capacitative calcium entry revisited. [Review] [55 refs]. *Cell Calcium* **11,** 611-24.

Robinson, I. M., and Burgoyne, R. D. (1991). Characterisation of distinct inositol 1,4,5-trisphosphate-sensitive and caffeine-sensitive calcium stores in digitonin-permeabilised adrenal chromaffin cells. *Journal of Neurochemistry* **56,** 1587-93.

Sagara, Y., and Inesi, G. (1991). Inhibition of the sarcoplasmic reticulum Ca^{2+} transport ATPase by thapsigargin at subnanomolar concentrations. *Journal of Biological Chemistry* **266,** 13503-6.

Sayers, L. G., Brown, G. R., Michell, R. H., and Michelangeli, F. (1993). The effects of thimerosal on calcium uptake and inositol 1,4,5-trisphosphate-induced calcium release in cerebellar microsomes. *Biochemical Journal* **289,** 883-7.

Schultz, R. M., and Kopf, G. S. (1995). Molecular basis of mammalian egg activation. [Review] [186 refs]. *Current Topics in Developmental Biology* **30,** 21-62.

Shiraishi, K., Okada, A., Shirakawa, H., Nakanishi, S., Mikoshiba, K., and Miyazaki, S. (1995). Developmental changes in the distribution of the endoplasmic reticulum and inositol 1,4,5-trisphosphate receptors and the spatial pattern of Ca^{2+} release during maturation of hamster oocytes. *Developmental Biology* **170,** 594-606.

Sudhof, T. C., Newton, C. L., Archer, B. 3., Ushkaryov, Y. A., and Mignery, G. A. (1991). Structure of a novel $InsP_3$ receptor. *EMBO Journal* **10,** 3199-206.

Sugiyama, T., Yamamoto-Hino, M., Miyawaki, A., Furuichi, T., Mikoshiba, K., and Hasegawa, M. (1994). Subtypes of inositol 1,4,5-trisphosphate receptor in human hematopoietic cell lines: dynamic aspects of their cell-type specific expression. *FEBS letters* **349,** 191-196.

Sun, F. Z., Hoyland, J., Huang, X., Mason, W., and Moor, R. M. (1992). A comparison of intracellular changes in porcine eggs after fertilization and electroactivation. *Development* **115,** 947-56.

Supattapone, S., Worley, P. F., Baraban, J. M., and Snyder, S. H. (1988). Solubilization, purification, and characterization of an inositol trisphosphate receptor. *Journal of Biological Chemistry* **263,** 1530-1534.

Swann, K. (1990). A cytosolic sperm factor stimulates repetitive calcium increases and mimics fertilization in hamster eggs. *Development* **110,** 1295-302.

Swann, K. (1991). Thimerosal causes calcium oscillations and sensitizes calcium-induced calcium release in unfertilized hamster eggs. *FEBS Letters* **278,** 175-8.

Swann, K. (1992). Different triggers for calcium oscillations in mouse eggs involve a ryanodine-sensitive calcium store. *Biochemical Journal* **287,** 79-84.

Tahara, M., Tasaka, K., Masumoto, N., Mammoto, A., Ikebuchi, Y., and Miyake, A. (1996). Dynamics of cortical granule exocytosis at fertilization in living mouse eggs. *American Journal of Physiology* **270,** C1354-61.

Takemura, H., Hughes, A. R., Thastrup, O., and Putney, J., Jr. (1989). Activation of calcium entry by the tumor promoter thapsigargin in parotid acinar cells. Evidence that an intracellular calcium pool and not an inositol phosphate regulates calcium fluxes at the plasma membrane. *Journal of Biological Chemistry* **264,** 12266-71.

Tesarik, J., Sousa, M., and Mendoza, C. (1995). Sperm-induced calcium oscillations of human oocytes show distinct features in oocyte center and periphery. *Molecular Reproduction and Development* **41,** 257-63.

Thastrup, O., Cullen, P. J., Drobak, B. K., Hanley, M. R., and Dawson, A. P. (1990). Thapsigargin, a tumor promoter, discharges intracellular Ca^{2+} stores by specific inhibition of the endoplasmic reticulum Ca^{2+}-ATPase. *Proc Natl Acad Sci U S A* **87,** 2466-70.

Turner, P. R., Jaffe, L. A., and Fein, A. (1986). Regulation of cortical vesicle exocytosis in sea urchin eggs by inositol 1,4,5-trisphosphate and GTP-binding protein. *Journal of Cell Biology* **102,** 70-6.

Van Blerkom, J. (1981). Structural relationship and posttranslational modification of stage-specific proteins synthesized during early preimplantation development in the mouse. *Proc Natl Acad Sci U S A* **78,** 7629-33.

Whitaker, M., and Swann, K. (1993). Lighting the fuse at fertilization. *Development* **117,** 1-12.

Whitaker, M. J., and Steinhardt, R. A. (1982). Ionic regulation of egg activation. *Quarterly Reviews of Biophysics* **15,** 593-666.

Wictome, M., Michelangeli, F., Lee, A. G., and East, J. M. (1992). The inhibitors thapsigargin and 2,5-di(*tert*-butyl)-1,4-benzohydroquinone favour the E2 form of the Ca^{2+},Mg^{2+}-ATPase. *FEBS Letters* **304,** 109-13.

Xu, Z., Lefevre, L., Ducibella, T., Schultz, R. M., and Kopf, G. S. (1996). Effects of calcium-BAPTA buffers and the calmodulin antagonist W-7 on mouse egg activation. *Developmental Biology* **180,** 594-604.

Yamada, N., Makino, Y., Clark, R. A., Pearson, D. W., Mattei, M. G., L., G. J., Ohama, E., Fujino, I., Miyawaki, A., Furuichi, T., and Mikoshiba, K. (1994). Human inositol 1,4,5-trisphosphate type 1 receptor, $InsP_3R1$: structure, function, regulation of expression and cromosomal localization. *Biochemical Journal* **302,** 781-790.

Yamamoto-Hino, M., Sugiyama, T., Hikichi, K., Mattei, M. G., Hasegawa, K., Sekine, S., Sakurada, K., Miyawaki, A., Furuichi, T., Hasegawa, M., and Mikoshiba, K. (1994). Cloning and characterization of human type 2 and type 3 inositol 1, 4, 5-trisphosphate receptors. *Receptors and Channels* .

Yoshikawa, S., Tanimura, T., Miyawaki, A., Nakamura, M., Yuzaki, M., Furuichi, T., and Mikoshiba, K. (1992). Molecular cloning and characterization of the inositol 1,4,5-trisphosphate receptor in Drosophila melanogaster. *Journal of Biological Chemistry* **267,** 16613-9.

Acknowledgement

I wish to acknowledge with deep appreciation the generous supervision of Drs. Katsuhiko Mikoshiba and Teiichi Furuichi. I would like to express my extreme gratitude to Drs. Sadahiro Azuma (Mitsubishi Kasei Institute of Life Sciences) and Yukako Kuroda (Keio University, School of Medicine) for continuous encouragement and invaluable discussion throughout this study. At last, I would like to thank all the members in Mikoshiba laboratory especially to Dr. Miki Yamamoto-Hino and Tohru Kokubo for continuous support and fruitful discussion.

February 1998

Kei Suga

Kei Suga

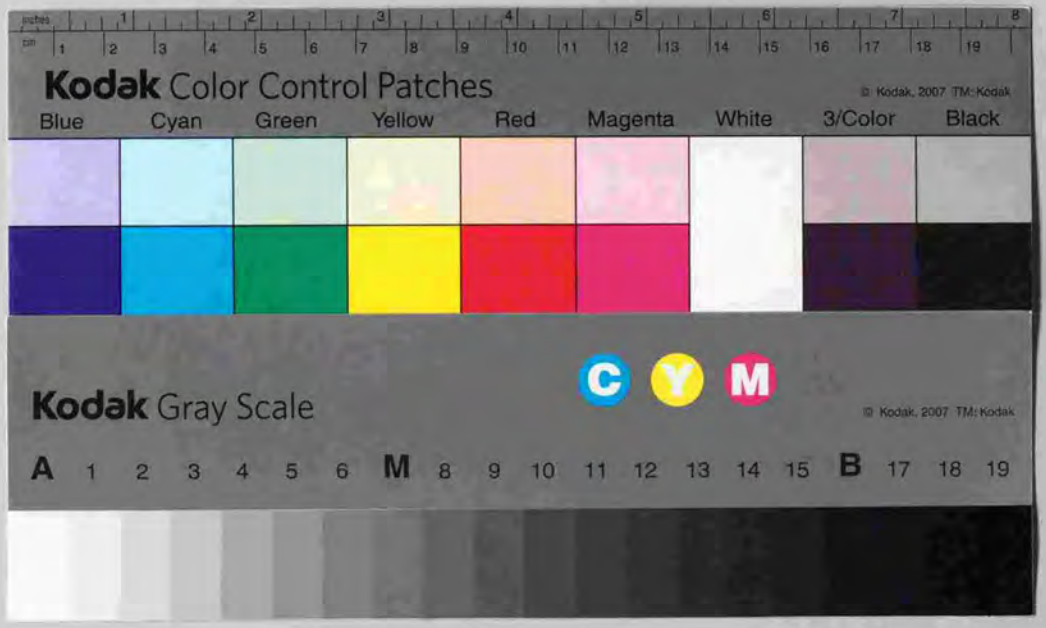
inches
cm
Kodak Color Control Patches
© Kodak, 2007 TM: Kodak
Blue
Cyan
Green
Yellow
Red
Magenta
White
3/Color
Black
Kodak Gray Scale
C
Y
M
© Kodak, 2007 TM: Kodak
A 1 2 3 4 5 6 M 8 9 10 11 12 13 14 15 B 17 18 19